Spring 2015

Spectral broadening of frequency combs via pulse apodization prior to nonlinear propagation

Oscar E. Sandoval
Purdue University

Graduate School Form 30
(Revised 08/14)

PURDUE UNIVERSITY
GRADUATE SCHOOL
Thesis/Dissertation Acceptance

This is to certify that the thesis/dissertation prepared

By Oscar Sandoval

Entitled
Spectral Broadening of Frequency Combs Via Pulse Apodization Prior To Nonlinear Propagation

For the degree of Master of Science in Electrical and Computer Engineering

Is approved by the final examining committee:

ANDREW M. WEINER

DANIEL S. ELLIOTT

PETER A. BERMEL

To the best of my knowledge and as understood by the student in the Thesis/Dissertation Agreement, Publication Delay, and Certification/Disclaimer (Graduate School Form 32), this thesis/dissertation adheres to the provisions of Purdue University's "Policy on Integrity in Research" and the use of copyrighted material.

ANDREW M. WEINER

Approved by Major Professor(s):

Approved by: Michael R. Melloch 04/27/2015

Head of the Department Graduate Program Date

SPECTRAL BROADENING OF FREQUENCY COMBS VIA PULSE APODIZATION PRIOR TO NONLINEAR PROPAGATION

A Thesis

Submitted to the Faculty

of

Purdue University

by

Oscar E. Sandoval

In Partial Fulfillment of the

Requirements for the Degree

of

Master of Science in Electrical and Computer Engineering

May 2015

Purdue University

West Lafayette, Indiana

This work is dedicated to my parents, Oscar and Georgina Sandoval for their love and guidance. To my brother Jesse Sandoval for his friendship and respect. *Para Nato y mi Mamaita, por haberme enseñado que es ser un hombre cabal.* To my aunts, uncles, and cousins whose constant support kept me motivated. To my girlfriend Katie Hummel for her companionship and support during the writing of this work. To James Brendan Hagan for becoming my best friend here at Purdue. To Dr. Eric Lara for seeing something in me when others didn't. And to those dreamers like me in East Los Angeles, CA. May this work serve as a testament that through hard work and empathy dreams come true.

What's Next?

ACKNOWLEDGMENTS

I would like to thank Professor Weiner for treating me with empathy. Dr. Dan Leaird for his invaluable input. AJ Metcalf for his mentorship and patience. Dr. Hyoung-Jun Kim for his advice. And all the members of the Ultrafast Optics and Optical Fiber Communications Laboratory.

TABLE OF CONTENTS

Page

LIST OF TABLES

LIST OF FIGURES

Figure Page

ABBREVIATIONS

DDF	Dispersion Decreasing Fiber
HNLF	Highly Nonlinear Fiber
SSFM	Split Step Fourier Method
NLSE	Nonlinear Schrodinger Equation
ASC	Adiabatic Soliton Compression
SPM	Self Phase Modulation
GVD	Group Velocity Dispersion
CEO	Carrier Envelope Offset
MLL	Mode Locked Laser
OAWG	Optical Arbitrary Waveform Generation
EDFA	Erbium Doped Fiber Amplifier
OSA	Optical Spectrum Analyzer
AC	Autocorrelation
CW	Continuous Wave
MSSR	Main to Secondary Sidelobe Ratio
FIR	Finite Inpulse Response
FSR	Free Spectral Range
FWHM	Full Width Half Maximum
OWB	Optical Wave Breaking
TBP	Time Bandwidth Product

ABSTRACT

Sandoval, Oscar E. M.S.E.C.E., Purdue University, May 2015. Spectral Broadening of Frequency Combs Via Pulse Apodization Prior to Nonlinear Propagation. Major Professor: Andrew M. Weiner.

This thesis focuses on specific methods for spectrally broadening large repetition rate frequency combs using the idea that tailoring the shape of the seed pulse prior to nonlinear propagation will result in a spectrally flatter comb. A spectrally flat comb is desired for applications in optical communications, arbitrary waveform generation, and microwave photonic filtering. Three experimental setups using Fourier transform pulse shapers, Dispersion Decreasing Fiber (DDF) or Highly Nonlinear Fiber (HNLF) as the nonlinear propagation media were performed. Simulations employing the Split Step Fourier Method to solve the Nonlinear Schrodinger Equation were performed to analyze the experimental results. The first experiments employed DDF to produce a compressed pulse via Adiabatic Soliton Compression. This pulse was launched into the second stage and HNLF broadened the comb spectrum via Self Phase Modulation. A promising 130nm broadened comb spectrum was returned. The next experiments showed that, by apodizing the pulse produced by the optoelectronic frequency comb generator prior to propagation in HNLF, a flatter broadened comb spectrum was returned. These results were extended to a two-stage setup. The setup used two stages of HNLF. $Sech^2$ apodization in the first stage and parabolic apodization in the second stage led to promising simulation results. With the insight gained by the simulations, experiments were performed and a flat broadened frequency comb led to applications in RF photonic filtering. An RF photonic phase filter was implemented with the comb generated as the source, and pulse compression experiments were performed.

1. INTRODUCTION

A frequency comb is a light source whose spectrum consists of a set of evenly spaced frequency components with a coherent and stable phase relationship [1]. Frequency combs have piqued interest in many fields including metrology [2], optical communications [3–5], radio frequency photonics [6–9] , and arbitrary waveform generation [10]. For applications in spectroscopy, a frequency comb with high precision and accuracy is needed. This type of comb can be achieved by stabilizing the pulse train generated by a mode locked laser (MLL). The visualization of this can be seen in figure 1.1. The time domain corresponds to a train of short optical pulses. The frequency domain is then the Fourier transform of the pulses and returns a series of frequency components looking similar to Dirac delta functions. In 2005, Hänsch and Hall shared the Nobel Prize for their work performed in determining the absolute frequency of the individual components. If the pulses generated by the laser were identical, then the absolute positions of the spectral components would be integer multiples of the laser repetition rate. However, due to dispersion and nonlinearities, there is a slip known as the Carrier Envelope Offset (CEO) due to the constant shifts in the oscillations of the electric field with respect to the pulse envelope. Therefore the equation for the frequency of each spectral component is given by equation 1.1.

$$f(n) = f_o + n f_{rep} \tag{1.1}$$

f_o is the offset frequency caused by the CEO, f_{rep} is the repetition rate of the laser which is the inverse of the round trip time, and n is an integer. If a comb that is an octave in bandwidth is available, that is a comb whose highest frequency must be at least double the lowest frequency, self-referencing can be employed to determine the value of f_o. A mode on the low frequency side of the spectrum is doubled. Now

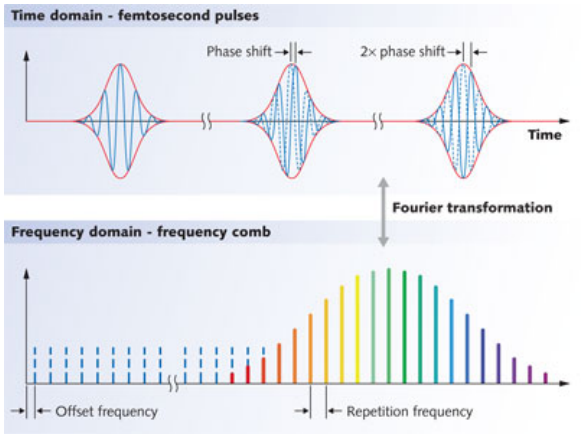

(a) Cartoon of frequency comb in time and frequency domains [11]

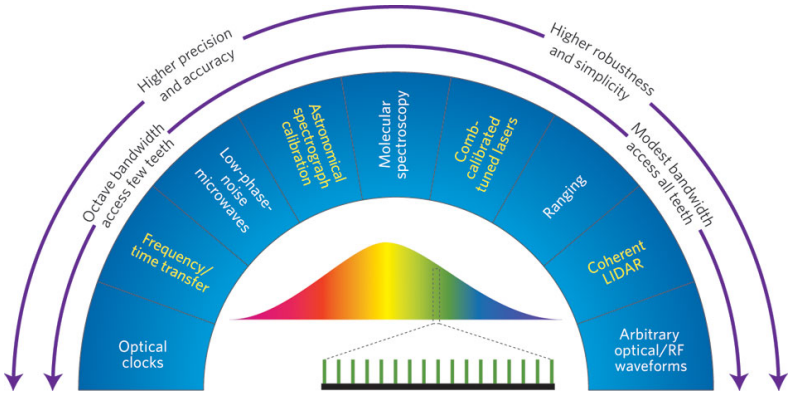

(b) Cartoon of applications of frequency combs [12]

Fig. 1.1. a. Figure of cartoon of frequency combs showing train of pulses in the time domain and the corresponding frequency components resembling dirac delta functions in the frequency domain. b. application wheel showing the applications of the different flavors of combs.

there is a mode on the high frequency side of the spectrum corresponding to the low frequency mode. Beating this new frequency doubled mode with the nearest high frequency mode allows the CEO to be determined.

These self-referenced combs are useful for the aforementioned applications when high precision and accuracy are needed. These applications fall in the left side of the wheel in figure 1.1b. However, these types of combs typically have a repetition

rate below 1GHz. Therefore, for applications in optical communications, arbitrary waveform generation, and RF photonic filtering, a different flavor of comb is desired. These applications fall on the right side of the application wheel in figure 1.1b. These types of combs are known as EO combs and possess flexibility in tuning the repetition rate, center wavelength, and optical bandwidth. By employing repetition rates higher than 1GHz, this allows for spectrally resolving the individual lines known as line-by-line shaping. These types of combs can lead to a robust solution that is cost-effective and can work outside of the laboratory. However, these types of combs are not as broad as the higher precision combs, but methods exist to broaden their spectrum. An example of a method for spectral broadening is to place a modulator in a laser cavity [13]. The drawback of spectrally broadening these so-called electro-optic combs is that their spectrum is not flat after broadening. A spectrally flat comb is one in which its spectral components have equal power. These spectrally flat combs are desired for channel equalization in optical communications and for pulse shaping. This thesis will focus on specific methods for spectrally broadening these electro-optic frequency combs using the idea that, by tailoring the shape of the seed pulse prior to nonlinear propagation, this will result in a spectrally flatter comb.

1.1 Spectral Broadening

Spectral broadening involves launching a high intensity pulse through a highly nonlinear fiber (HNLF). There are two types of dispersion in HNLF, Anomalous and Normal. Both of these types of dispersion will be discussed in greater detail in the following sections of the introduction and the following chapters in this thesis, but here they will be briefly introduced. In anomalous dispersion, the process at work is Adiabatic Soliton Compression (ASC). This results in a compressed soliton pulse at the output. However, this requires precise control of the length of the fiber and input intensity of the pulse. Normal dispersion is more stable and an increase in power will result in an increase in bandwidth. However, after propagation in a distance of fiber,

the pulse will broaden due to the interplay of group velocity dispersion (GVD) and self phase modulation (SPM) which leads to a quadratic chirp. GVD is the effect of the different frequency components making up the pulse traveling at different velocities. SPM is the physical process of a change in phase of an optical pulse due to the nonlinearity of the refractive index of the medium of propagation [14]. SPM stems from the optical Kerr effect, which is a change in refractive index arising from an applied electric field. Because SPM arises and leads to spectral broadening in both the normal and anomalous dispersion regimes, it is introduced here in more depth.

1.1.1 Self Phase Modulation

The following derivation is based on [14]. The nonlinear refractive index is given by equation 1.2

$$\mathrm{n}(t) = \mathrm{n}_o + \mathrm{n}_2 I(t) \tag{1.2}$$

where the intensity of the pulse is $I(t) = 2\mathrm{n}_o\epsilon_o c|A(z,t)|^2$. The effect this has on the pulse is that it induces a time varying phase denoted $\phi_{NL}(t)$ in equation 1.3.

$$\phi_{NL}(t) = -\mathrm{n}_2 I(t)\omega_o \frac{L}{c} \tag{1.3}$$

This time varying phase results in the spectrum of the pulse to be modified [14]. This modification usually leads to broadening. An intuitive way of describing the spectrum is to analyze the instantaneous frequency of the pulse which is given by equation 1.4.

$$\omega(t) = \omega_o + \delta\omega(t) \tag{1.4}$$

In equation 1.4, $\delta\omega(t)$ is the variation of the instantaneous frequency.

$$\delta\omega(t) = \frac{d}{dt}\phi_{NL}(t) \tag{1.5}$$

By employing both equations 1.4 and 1.5 the frequency components corresponding to the trailing and leading edge of the pulse can be characterized. Figure 1.2 shows an example of a pulse and its instantaneous frequency.

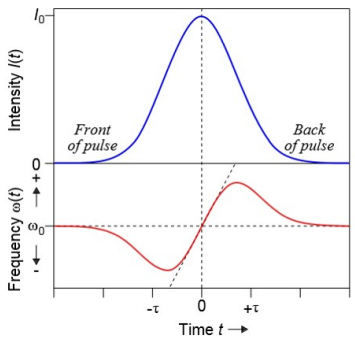

Fig. 1.2. Example of a pulse and the corresponding instantaneous frequency. The instantaneous frequency depicts the characterization of the frequency components, in this case under the effect of normal dispersion [15].

From [16] if SPM is not present in the system and $D = 0$, this will result in pulses that are chirp free. A chirp will be induced if $D \neq 0$. The sign of the chirp is dependent on the sign of the dispersion. If SPM is present in the system, the sign of the dispersion plays a crucial role on the behavior of the pulse. To denote anomalous or normal dispersion, the dispersion parameter D is introduced. The units expressed in terms of wavelength are $ps/nm/km$. For normal dispersion, $D < 0$. For anomalous dispersion, $D > 0$ [17]. If $D = 0$, the pulses are up-chirped and this leads to generation of short pulses and more bandwidth when compared to the case when SPM is not present in the system and $D = 0$. This is an important characteristic because it is this that leads to the generation of new frequency components, i.e. spectral broadening.

1.2 Anomalous vs Normal Dispersion

It is important to understand what is meant when anomalous or normal dispersion is mentioned. In normal dispersion, the higher frequency components travel slower than the lower frequency components. That is to say the leading edge of the pulse is red shifted and the trailing edge of the pulse is blue shifted.

In anomalous dispersion, the higher frequency components travel faster than the lower frequency components. That is to say the leading edge of the pulse is blue shifted and the trailing edge of the pulse is red shifted.

Here the explanation from [16] of the effects SPM has when the dispersion is either normal or anomalous is continued. When $D > 0$, the SPM and GVD both individually lead to an up-chirp. The frequency components in the leading edge of the pulse are down-shifted, i.e red shifted, because of SPM. And the normal GVD shifts these frequency components to an earlier time. Furthermore, due to SPM the frequency components in the trailing edge of the pulse are up-shifted. And the normal GVD shifts these frequency components to a later time. When both GVD and SPM act on the pulse, this leads to faster temporal broadening and more chirping is induced when compared to the case when only GVD acts on the pulse. The important characteristic that should be noted is that for a fixed dispersion value D, the bandwidth increases when the SPM increases. When $D < 0$, SPM leads to an up-chirp and GVD leads to a down-chirp. These two effects can balance each other, and when this occurs a Soliton arises. More information will be provided on both of these cases in the following sections.

Work has been done in trying to obtain a flatter comb during the spectral broadening process. To do this, the input pulse is apodized (shaped) prior to nonlinear propagation. In the following sections of this thesis, the main principle will be applied. A pulse will be shaped prior to nonlinear propagation to return a flat broadened comb spectrum. Different pulse shapes will be presented.

[18, 19] showed that multiple stages of pulse apodization lead to a flat spectral profile. In these experiments, specialized components were employed to result in a flat spectral broadening.

In the Section 2.0, a simpler scheme is presented for achieving a flat spectral profile. The scheme employs commercially available HNLF, Dispersion Decreasing Fiber, and Fourier Transform pulse shapers.

1.3 Adiabatic Soliton Compression in Dispersion Decreasing Fiber

The first stage in experimental setup in section two employs Dispersion Decreasing Fiber (DDF) to return a compressed pulse that can be launched into the second stage. DDF is fiber whose dispersion slowly decreases [16]. These fibers are made by tapering the core of silica-based fibers during the pulling process [20]. These fibers can be used to compress soliton pulses [20]. A soliton pulse maintains its shape as it propagates through fiber [16]. This can be better understood by examining the equation that governs the adiabatic soliton compression phenomena.

$$\frac{T(z)}{T(0)} = \frac{\beta_2(z)}{\beta_2(0)} \tag{1.6}$$

$T(0)$ is the input pulse width and $\beta_2(0)$ is the input dispersion value. Both of these parameters are held constant. As the pulse propagates through the fiber, the dispersion $\beta_2(z)$ decreases. In order for the equation governing this process to hold true, the pulse width $T(z)$ must also decrease.

Another way to look at this is by analyzing the following relationship.

$$\text{Energy of Pulse} \rightarrow \text{Pulse width} \rightarrow \frac{GVD}{\gamma} \tag{1.7}$$

The energy of the pulse and the nonlinear parameter γ are held constant. Note that γ is the nonloinearity of the fiber. If the GVD is decreased, then the pulse width must also decrease. Using DDF to perform ASC will return a compressed pulse of high quality and little energy in its wings [16]. But how exactly does the DDF compress the soliton pulse? DDF has anomalous group velocity dispersion. As a pulse propagates through the fiber, it experiences SPM. The anomalous GVD and the SPM work to counteract each other. Therefore as the pulse propagates through the fiber, the soliton keeps it shape [21].

1.4 Spectral Broadening in Highly Nonlinear Fiber

In the following experimental setups, HNLF is used to broaden the comb spectrum. HNLF can be used in various applications ranging from wavelength conversion to Raman amplification to optical switching, and supercontinuum generation [22]. It has been shown that when a high peak power pulse propagates in optical fiber, its spectrum is broadened [22]. The SPM is responsible for spectral broadening. In HNLF, the SPM and the normal GVD work to complement each other to induce temporal pulse broadening [16].

The following description is adapted from [16]. Initially, SPM is the dominant physical phenomena leading to spectral broadening. As propagation continues, GVD begins to play a stronger role. Then broadening occurs in the temporal domain. As temporal pulse broadening occurs, the intensity of the pulse is reduced. As the intensity is reduced, the spectral broadening continues but not as rapidly.

1.4.1 Chirped Pulse

Here it is important to understand what is meant when a pulse is said to be chirped and what is meant when a pulse is said to be simultaneously bandwidth limited and free of phase modulation. The following explanation is derived from [16].

$$a(t) = |a(t)|\mathrm{e}^{j\phi(t)} \tag{1.8}$$

$$A(\omega) = |A(\omega)|\mathrm{e}^{j\Phi(\omega)} \tag{1.9}$$

Equation 1.8 represents the optical pulse in the time domain and equation 1.9 represents the pulse in the frequency domain. When a pulse is said to be "free of phase or frequency modulation" this means that $\phi(t)$ is held constant. When a pulse is said to be bandwidth limited, this means that $\Phi(\omega)$ is held constant.

When a pulse is simultaneously bandwidth limited and free of phase modulation, this means $\Phi(\omega) = 0$ and $\phi(t) = 0$. However, if $\Phi(\omega)$ and $\phi(t)$ both have a nontrivial variation, the pulse is chirped.

As stated above, the temporal broadening occurs due to the GVD. If there is a long propagation, GVD becomes the dominant effect. If there is no GVD in the fiber and only SPM was the physical phenomena present, then there would be no temporal broadening and only spectral broadening. So how do we compensate for the GVD and temporal broadening it induces?

1.4.2 How Is A Chirped Pulse Compensated For After HNLF Propagation

As stated in [16], when GVD is positive and sufficiently large, SPM and GVD work in concert and lead to a substantially linear chirp. This linear chirp, or quadratic spectral phase, can easily be compensated with a SMF or a Fourier Transform pulse shaper. Note that this is not the only method to compensate for the chirp induced on the pulse. Dispersion compensating fiver (DCF) can be used to compensate for chirp, and single mode fiber (SMF) can be used to compensate for linear chirp.

The second order dispersion is given by equation 1.10 and the variable ϕ_2 used in programming the pulse shaper, is given by equation 1.11. Here z is the length of fiber.

$$\beta_2 = -\frac{D\lambda^2}{2\pi c} \tag{1.10}$$

$$\phi_2 = z\beta_2 \tag{1.11}$$

Equation 1.12 is the transfer function used for application of phase.

$$H(\omega) = \mathrm{e}^{j\frac{\phi_2}{2}(2\pi f)^2} \tag{1.12}$$

Higher order dispersion parameters can be added by simply altering the transfer function. By altering the value of z and the sign of the phase, this will either compress the pulse or spread the pulse more.

1.5 Pulse Shaping

To understand how the shaping is done, a brief overview of pulse shaping is introduced here.

Temporally nondispersive grating and lens apparatus [23], or better known as a pulse shaper, allows for the tailoring of femtosecond optical pulses into arbitrary shapes. The basic concept of a pulse shaper is that it is possible to control the amplitude and the phase of the different frequency components that make up a pulse. This is done by using a mask. An amplitude mask controls the amount of light that is transmitted through. And a phase mask controls the time it takes the different frequency components from traveling through the mask. The basic principle of pulse shaping consists of the input light to disperse off the first grating. This spreads the spectrum so that the different wavelengths that make up the pulse travel in slightly different directions. The first lens then focuses the dispersed wavelengths onto the mask. The second lens then focuses the wavelengths onto the grating that then recombines the different wavelengths into one collimated beam.

1.6 Simulations Using Split Step Fourier Method

To perform pulse propagation in nonlinear fibers, the Split Step Fourier Method (SSFM) is employed to numerically solve the Nonlinear Schrödinger Equation (NLSE). The NLSE has been shown to govern pulse propagation in lossless fiber with second order dispersion [24]. This is because the second-order derivative represents the dispersion and the nonlinearity is represented by γ. This allows for modeling nonlinear effects in the fiber.

$$i\frac{\partial u}{\partial z} - \frac{\beta_2}{2}\frac{\partial^2 u}{\partial t^2} + \gamma|u|^2 u = 0 \tag{1.13}$$

In equation 1.9, u is the complex field envelope, z is the propagation distance, and β_2 is the second order dispersion. The NLSE can be modified to include effects from other physical phenomena such as fiber loss, third order dispersion, amplification, amplified spontaneous emission noise, and polarization mode dispersion [16, 24–27]. However, in most cases an analytical solution cannot be found.

SSFM is the most popular way to solve the NLSE when there is no exact solution available. The SSFM treats the linear and nonlinear characteristics of the optical fiber separately [16]. The nonlinear terms are dealt with in the time domain, and the linear terms are dealt with in the frequency domain. And because SSFM employs Fourier and inverse Fourier transforms to go between the time and frequency domains, it is computationally efficient. Some precautions must be taken to ensure the simulations return accurate results. Error is introduced in the simulations because SSFM ignores the noncommuting nature of the dispersion and nonlinearities. In order to minimize this error, a small step size should be selected. The length of the time and frequency vectors must be initialized so that the sampling is accurate. This is analogous to ensuring the time and frequency vectors accommodate the size of the pulse and spectrum respectively [16].

1.7 Organization of Thesis

The remainder of this thesis is organized as follows. Section 2.0 will present a two stage broadening technique and the physics involved in both stages. Section 3.0 delves deeper into shaping the pulse prior to nonlinear propagation that will result in a flatter broadened comb spectrum. In Section 4.0, a two stage HNLF broadening technique is presented and the generated broadened comb will be used in RF photonic phase filtering. Finally, Section 5.0 will briefly summarize the thesis

2. PULSE APODIZATION IN TWO STAGES OF NONLINEAR PROPAGATION

It has been previously reported that altering the seed pulse prior to each stage of nonlinear propagation can result in a broad and spectrally flat comb [18, 19]. It is from these multiple stage techniques that the following experiments are implemented. In the work presented in this section, straightforward techniques with commercially available components are used to spectrally broaden the seed comb.

It must be noted that this will not be an easy task. In order to achieve similar results to those reported in [18, 19] such adverse effects like nonlinear phase, spectral ripple, and ASE noise must be dealt with.

After nonlinear spectral broadening, the edges of the spectrum will have acquired some nonlinear phase. This phase cannot be compensated by the use of SMF. This will leave some residual phase that will lead to a degradation in achievable bandwidth and spectral flatness of the broadened comb spectrum in the second stage. Solutions proposed to the residual phase problem include applying a band pass filter [28], employing the use of a pulse shaper [29], and applying the technique known as Chirped Pulse Amplification [30].

If the spectrum is windowed using a band pass filter, this will essentially remove the wings of the broadened spectrum [28]. This solution proposes to remove bandwidth which was difficult to produce. A pulse shaper can be used to correct the residual phase. Using the pulse shaper can also be used to tailor the spectrum prior to nonlinear propagation. However, the maximum input power of the pulse shaper must be taken into consideration in order to prevent damage. This will determine the order in which the pulse shaper and the high-power amplifier are placed. This will be explained further in the discussion section of this chapter. Using the pulse shaper to pre-compensate for the nonlinear phase induced by propagation in the high

power EDFA and HNLF is a complicated process. Performing this pre-compensation requires the use of iterative feedback loops and complex algorithms such as covariance matric adaptation evolution strategy CMA-ES [31]. Alternatively, by reducing the peak intensity of the input pulse, this results in a reduction of nonlinear interactions. This process is known as CPA [16].

To reduce the peak intensity, the pulse is stretched. SMF can be used to achieve this stretching by applying a chirp. When the stretched pulse is launched into the amplifier, the reduced peak intensity results in less nonlinearities from the amplifier adversely affecting the pulse. The most difficult part of the CPA process is the compression of the pulse after the amplifier. If the pulse is not completely compressed, this will result in degradation of the broadened comb spectrum. CPA also does not allow for ASE noise that the amplifier induces to the system to be rectified.

The first stage of the proposed setup uses a source that requires little manipulation. In [32] the spectral and temporal domain output of an optoelectronic pulse broadened in both normal dispersion HNLF and DDF were compared. It has also been reported that DDF produces a clean pulse shape that is nearly wing free [20, 21, 33]. The advantageous characteristic of a pulse generated from DDF is that it is compressed without the need of additional dispersion compensation.

Therefore the proposed setup employs DDF in the first stage. This broadens the input spectrum and creates a compressed wing free pulse to be launched into the second stage. This stage employs normal dispersion HNLF for nonlinear spectral broadening. In the following section DDF will be explored more in depth.

2.1 Dispersion Decreasing Fiber

In order to better understand the physical phenomenon that results in this type of fiber, it is important to understand the type of pulse known as Solitons. A Soliton is a pulse that can propagate without undergoing any distortion from the joint effect of nonlinearity and dispersion [16]. The Soliton can be thought of as the natural

optical bit. Solitons arise in the anomalous dispersion regime. This is because in anomalous dispersion, SPM and GVD can work to counteract each other. When these two physical phenomena exactly compensate each other, the pulse that arises is a Soliton. However, for this to occur a specific power level must be achieved. The equation representing a Soliton is given in 2.1.

$$a(z,t) = \sqrt{P_c} sech(\frac{t}{T_o}) \mathrm{e}^{\frac{-j|\beta_2|z}{2T_o^2}} \tag{2.1}$$

The fundamental Soliton occurs only for special values of peak power P_c given by equation 2.2.

$$\frac{\gamma P_c T_o^2}{|\beta_2|} = 1 \tag{2.2}$$

The above equation was used to determine the power level needed to achieve a Soliton with a FWHM of T_o. Solving for P_c gives equation 2.3.

$$P_c = \frac{|\beta_2|}{\gamma T_o^2} \tag{2.3}$$

Now that the idea of a Soliton and the necessary power to achieve a soliton pulse is understood, the process known as adiabatic soliton compression (ASC) can be further explained. ASC is the physical phenomenon that leads to a compressed pulse. ASC is the manifestation of the robustness property of Solitons [16]. The robustness property is the ability of a system to resist change without adapting its initial stable condition. Studies have shown that a Soliton propagating in DDF is analogous to a Soliton propagating in a fiber with steady amplification [17]. In [16] it states that previous studies show that if the gain over one soliton period is small, this will cause the soliton to propagate adiabatically. This will cause the pulse duration to continually decrease as the energy of the soliton increases. The pulse duration after propagating is given by equation 2.4

$$\frac{U(z)}{U(0)} = G = \frac{T(0)}{T(z)} \tag{2.4}$$

U is the energy of the soliton pulse given by equation 2.5.

$$U = \frac{2|\beta_2|}{\gamma T_o} \tag{2.5}$$

Therefore, the Soliton is compressed with a compression factor of G known as the energy gain.

2.2 Experimental Setup

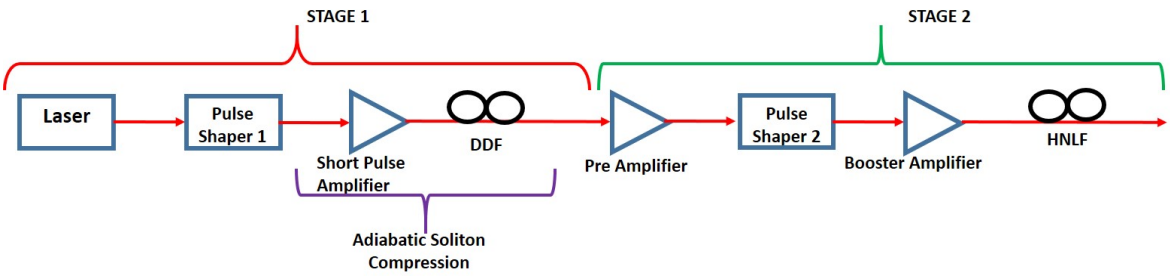

Fig. 2.1. Experimental setup for pulse apodization in two stages of nonlinear propagation experiments. In the first stage the short pulse amplifier and the DDF work in concert leading to ASC. In the second stage, HNLF is the nonlinear medium.

Figure 2.1 shows the experimental setup for the two stage broadening process. The first stage consists of the Laser, Pulse Shaper 1, Short Pulse Amplifier, and the DDF. The second stage then consists of the Pre-Amp of a High-Powered Amplifier, Pulse Shaper 2, the Booster Amp of the High-Powered EDFA and the HNLF. In the following section, the two stages and their respective components will be introduced and the purpose they serve will also be explained.

Stage 1

The Laser is an ERGO model manufactured by Time Bandwidth Products. It is a mode-locked laser (MLL) that outputs a Gaussian shaped spectral comb at a

repetition rate of 10GHz. The center wavelength of the laser is 1550nm. The pulse duration of the laser pulse is 2ps according to the specification sheet provided by the manufacturer and confirmed via experimental measurements.

The Pulse Shaper 1 is manufactured by Finisar. The pulse shaper works in the C-band (1527nm - 1567nm) and is used to apodize the Gaussian comb generated by the ERGO to a $sech^2$ shape. This allows for better pulse compression out of the DDF.

The Short Pulse Amplifier and the DDF work in concert to compress the pulse via ASC. As stated above, in order for a soliton pulse to be created the GVD and the SPM must completely balance each other. This occurs for specific values of peak power. 2km of commercially available DDF was used in this setup. The dispersion decreases linearly from $10ps/nm/km$ at the input to $1.5ps/nm/km$ at the output.

2.2.1 Stage 2

The Pre-Amp of the High-Powered EDFA achieves the threshold power necessary for amplification in the Booster Amplifier. The Pulse Shaper 2 is another commercially available pulse shaper. This pulse shaper is also manufactured by Finisar and works in the C-band (1527-1567nm). This pulse shaper applies quadratic phase to compensate for phase induced by propagation in fiber. The pulse shaper pre-compensates for the phase that will be induced by the Booster Amp and the SMF that leads to the HNLF. This allows for a compressed BW-Limited pulse to be launched into the HNLF. This is desired because a compressed pulse will lead to a higher peak intensity. A higher peak intensity will lead to more SPM to occur in the HNLF and this will lead to more spectral broadening.

The Booster-Amp is the second stage of the High-Powered EDFA. This amplifier works in concert with the HNLF to induce nonlinearities in the fiber. The power level of the Booster amplifier was set to 2W for these experiments unless otherwise stated.

The HNLF parameters are given in table 2.1.

Table 2.1.
Parameters for HNLF of length of 150m

Parameter	**Value**
Average Power	$P_{AVG} = 2W$
Length of Fiber	$z = 150m$
Dispersion Parameter	$D = -1.88ps/km/nm$
Nonlinear Coefficient	$\gamma = 10.5(Wkm)^{-1}$
Dispersion Slope	$S = 0.016ps/nm^2/nm$

2.3 Experimental Results

In order to better understand the experimental results, a step-by-step procedure followed by data will be presented. This will allow the reader to better comprehend what is occurring in the experiment, and will make the discussion section of this chapter easier to understand.

2.3.1 Stage 1

As mentioned before, the laser source is the ERGO MLL. Its output can be seen in figure 2.2a. The Bandwidth of the ERGO spectrum is 5nm within 10dB. The next step in the experimental procedure is to apodize the spectrum with the first pulse shaper. This will result in a spectrum with a $sech^2$ shape. The following is an explanation of the apodization technique. The pulse shaper takes a spectral trace of the spectrum from the OSA. The number of points that are above a certain power level are recorded. These points will be used in the apodization. All other points are set to a lower power level that is effectively zero. The target spectrum is formed and compared to the un-apodized spectrum. To form the target spectrum, the equation for the specific shape is used. The target spectrum and the un-apodized spectrum are plotted together in order to gain a better idea of how much of the spectrum is

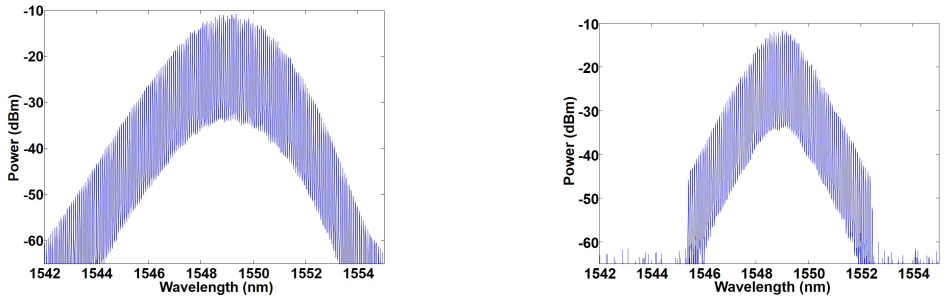

(a) Output spectrum of ERGO laser source.

(b) Sech^2 apodization.

Fig. 2.2. a. Figure of the 5nm wide Gaussian spectrum produced by the ERGO laser source; b. and the 3nm wide Sech^2 apodization.

being removed during the apodization process. Each peak is compared to the target peak value. The peak is then attenuated to fit the target spectrum. Multiple runs are done to achieve a spectrum that is close to the desired spectrum.

This new apodized spectrum has a bandwidth of 3nm and can be seen in figure 2.2b. This apodized spectrum is now seeded into the ASC section of the first stage. The pulse is launched into the short-pulse amplifier prior to the DDF. The power level of the amplifier is set to approximately 21dBm. The amplifier and the DDF work in tandem to achieve ASC; this was discussed previously. The output of the DDF is seen in figure 2.3a. The green spectrum in the figure is the simulated spectrum. This spectrum is used to simulate the broadening that will occur after propagation in HNLF of the second stage.

The spectrum of the pulse after the DDF is now 8nm wide. Notice the dip in the middle of the spectrum. This will lead to further discussion.

ASC leads to pulse compression. Therefore, the pulse that is launched into the ASC section of the first stage will be broader than the pulse outputted by this section. This is confirmed in figure 2.3b.

The autocorrelation of the pulse prior to the ASC section has a pulse width of approximately 2ps. Note, these are pulse widths estimated by applying the decon-

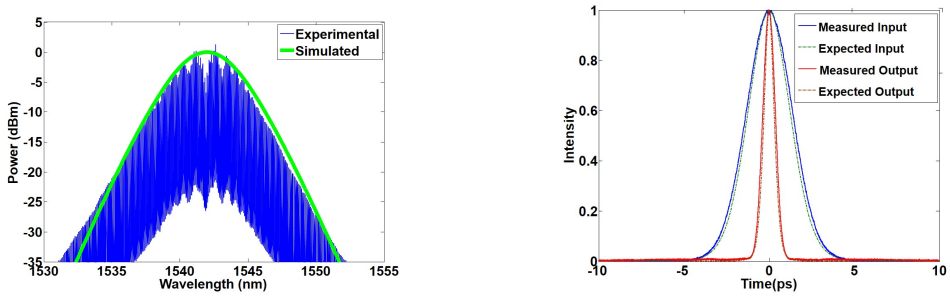

(a) Broadened spectrum at output of DDF.

(b) Comparison of autocorrelation traces launched and returned from the DDF.

Fig. 2.3. a. Figure of the 8nm broadened spectrum produced by the DDF; b. and the comparison of the autocorrelation traces launched and returned from the DDF. The AC traces demonstrate the pulse compression induced by ASC.

volution factor of 1.543 for a $sech^2$ shaped pulse. This is close to the ideal case of 1.92ps. This ideal case assumes no chirp, in other words a BW-limited pulse. After, the pulse propagates through the amplifier and the DDF ASC compresses the pulse. This results in a pulse width of approximately 660fs. This is close to the ideal case of 620fs. This confirms that the amplifier and the DDF are working in tandem to induce ASC. However, notice in figure 2.4 that the measured pulse after ASC has pedestals. That is to say that the pulse does not fully return to zero. This may result in degradation of the comb spectrum at the output of the second stage.

2.3.2 Stage 2

To ensure that a compressed pulse is launched into the HNLF, an autocorrelator is used. If the chirp on the pulse is completely compensated for by the pulse shaper, the pulse will be compressed. When the pulse is compressed, the intensity will be high. This can be analyzed by taking a trace of the spectrum from an OSA and taking an autocorrelation trace. The spectrum is then put through the Inverse

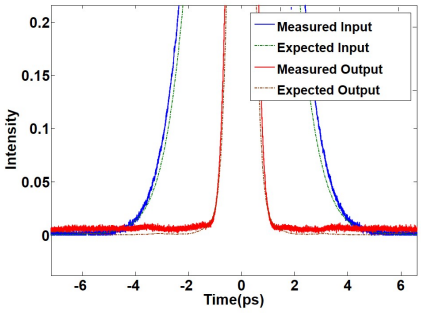

Fig. 2.4. Closer view of the temporal pedestals in the pulse after propagation in DDF.

Fourier Transform and this returns the intensity of the spectrum. However, this pulse intensity cannot be compared to the autocorrelation trace. Therefore, the spectrum intensity is self-convolved so as to return an autocorrelation trace. Now these two pulses can be compared. If the experimental autocorrelation trace is close to the ideal autocorrelation trace, it can be assumed that the bandwidth limited pulse is obtained and can be launched into the HNLF. In doing so, this will result in more spectral broadening. Note that this process is repeated whenever a compressed pulse is desired in experiments. Figure 2.5a shows the pulse that is launched into the HNLF.

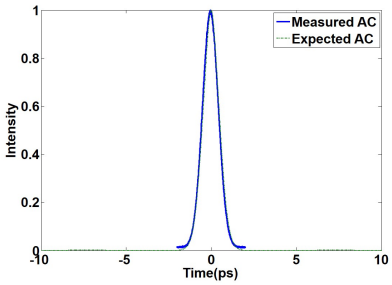

(a) Pulse launched into HNLF showing temporal pedestals.

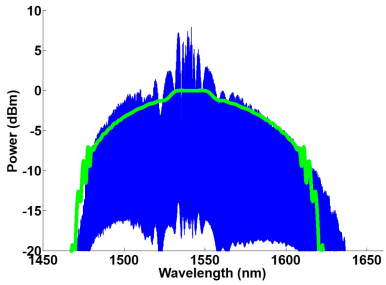

(b) Broadened spectrum produced by the HNLF with parameters listed in Table 2.1.

Fig. 2.5. a. Figure of the pulses launched into the HNLF; b. and the corresponding broadened spectrum. The broadened comb is 130nm wide within 10dB and corresponds to approximately 1600 lines.

Note that the pulse launched into the HNLF has the same temporal pedestals. This can be seen in figure 2.6.

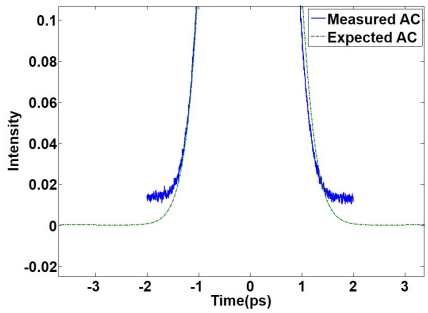

Fig. 2.6. Closer view of the temporal pedestals in the pulse that was launched into the HNLF.

This will result in degradation of the comb spectra and can be seen in figure 2.5b. This results in a comb that is 130nm wide looking within 10dB. This is an impressive amount of broadening. By performing the following calculation, the number of lines can be determined. In order to find the bandwidth in terms of frequency, equation 2.6 can be employed.

$$\Delta f = c\frac{\Delta\lambda}{\lambda^2} \tag{2.6}$$

In order to find the number of lines in the frequency comb, the bandwidth in terms of frequency is divided by the repetition rate of the laser.

$$\mathrm{N} = \frac{\Delta f}{f_{rep}} \tag{2.7}$$

The bandwidth in terms of frequency is calculated to be $1.62x10^{13}$Hz. Dividing this value by the repetition rate of the comb, 10GHz, gives that the number of lines is 1623. In equation 2.7 N is the number of lines.

The spectral ripple is relatively large. In this comb, it is over 10dB. As mentioned before, a flat comb spectrum is desired. Therefore, the amount of spectral ripple needs to be reduced. Recall that the pulse out of the DDF has temporal pedestals

that can also be seen in the compressed pulse that was launched into the HNLF. These temporal pedestals are thought to arise from the spectral depression that can be seen in figure 2.3a.

The power level of the short pulse amplifier was varied to return a smoother spectrum out of the DDF. Recall that a soliton is created when the GVD and the SPM in the fiber completely complement each other. This is done at a specific power level. So, by varying the power, the interplay between SPM and GVD is varied and the spectrum of the pulse out of the DDF may be made smoother.

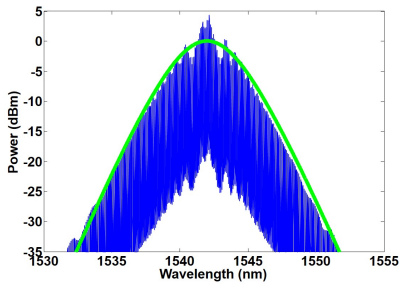

(a) Spectrum of smoother DDF broadening.

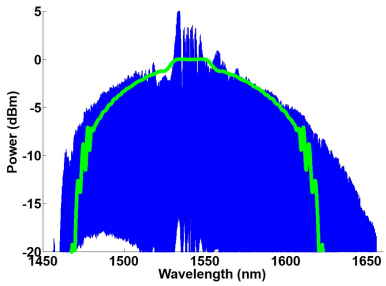

(b) Broadened spectrum after HNLF from the smoother DDF broadened spectrum.

Fig. 2.7. a. Figure of the smoother spectrum returned from the DDF; b. and the corresponding HNLF broadened comb spectrum. The new broadened spectrum is 175nm wide within 10dB and corresponds to 2100 lines.

Figure 2.7a shows the spectrum of the pulse after DDF and after the power on the short-pulse amplifier was reduced. This should result in a broader spectrum than the previous results that can be seen in figure 2.7b. The smoother DDF spectrum results in a smoother and broader comb spectrum after HNLF propagation. The comb is now 175nm wide, which results in 2185 lines. A reduction in spectral ripple is also evident.

To obtain a better perspective of the previous DDF spectrum and the most recent smoother spectrum, figure 2.8 is introduced.

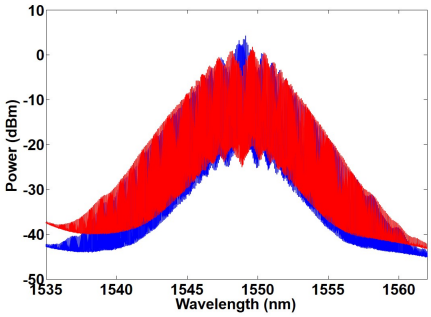

Fig. 2.8. Comparison of DDF spectra used during experiments. This figure shows the DDF spectrum with the spectral dip (red) and the removal of the spectral dip (blue) after varying the power in the short pulse amplifier.

It is clear that the most recent spectrum no longer has the spectral concavity in the middle. This may be the reason for a broader spectrum at the output of the second stage. However, it should be noted that the spectrum is still not entirely smooth. There still exist ripples in the spectrum. It is these power variations that cause temporal pedestals in the pulse, which in turn lead to power variations that are detrimental to the comb spectrum.

2.4 Discussion

The broadened comb spectrum is not flat because of the pulses launched into the HNLF. In order for a flat broadened spectrum to be generated, the pulses must be chirp free. This will ensure that the energy will be confined in the center of the pulse. Recall that the interplay of SPM and normal GVD will lead to a purely quadratic phase, i.e linear chirp. Therefore care must be taken to ensure that the pulses launched into the HNLF are chirp free.

2.4.1 Stage 1

The ERGO pulse is apodized to a $sech^2$ shape. This shape is chosen in order to help facilitate the soliton condition. Recall that the physical phenomena occurring in the DDF is ASC. A soliton has a $sech^2$ profile. Therefore, if the pulse is shaped to a soliton profile prior to DDF, ASC will be facilitated. A deviation from the soliton profile will results in degradation of the coherence and therefore result in more background noise being observed [32].

It would seem that the best location to place pulse shaper 1 would be after the amplifier. Thus compensating for the dispersion induced by propagation in the amplifier. However, the problem of power levels is then encountered. In order for ASC to take place, a certain power level must be achieved. If the pulse shaper is placed after the amplifier, the ASC power level will not be achieved. This is due to the fact that the pulse shaper introduces loss to the system. If the amplifier is set to the appropriate power level, after the pulse propagates through the pulse shaper the power level will be lower. The reader may then suggest to simply increase the amplifier until the appropriate power level at the output of the pulse shaper is achieved. However, then the maximum input power of the pulse shaper must be taken into account. The maximum input power of the pulse shaper is 27dBm. So, a better solution is to place to the pulse shaper prior to the amplifier and suffer the detrimental effects of ASE noise, rather than not achieving the appropriate power level for ASC to occur.

2.4.2 Stage 2

As stated before, the pulse shaper can be used to correct for residual phase. However, the maximum input power of the pulse shaper is 0.5W, and in order to achieve the amount of spectral broadening desired, the amplifier must be set to 2W. Therefore, if the pulse shaper is placed after the amplifier, the maximum power level the amplifier can be set to is 0.5W. But, not only is this not enough for spectral broadening in the second stage of HNLF, the pulse shaper will introduce loss and

the power level will be lower at the input of the HNLF leading to even less spectral broadening. So the amplifier must be placed prior to the amplifier. This is not ideal, because then the amplifier will alter the pulse spectrum after propagation through it and this will lead to degradation of the comb spectrum after HNLF propagation.

Apodizing the spectrum changes the amplitude of the spectral features. If this is done prior to the amplifier, then the amplifier will alter the newly apodized spectrum. In order to compensate for the phase the amplifier induces on the pulse, a feedback loop is required. These feedback loops are complicated and difficult to implement.

All this leads to the understanding that the quality of the pulse launched into the nonlinear medium is of utmost importance. If the pulse launched into the fiber is chirp free and compressed, this will lead to a flatter comb spectrum. However, if the pulse is not chirp free this leads to degradation in the flatness of the comb. Degradation in flatness makes it difficult to implement arbitrary waveform generation and make it difficult to implement channel equalization in optical communications. Therefore, this was an invaluable lesson to learn. This will be applied in the following experiments.

In summary, a 3nm wide $sech^2$ spectrum, within 10dB, is broadened to 130nm. A 175nm wide broadened comb spectrum within 10dB was achieved by obtaining a smoother spectrum after the DDF. Comparing this to [18, 19], more broadening is achieved. However, the spectral flatness of the broadened comb in this thesis, was not as flat. The power variation was $\leq$10dB for the 130nm wide comb, and $\leq$5dB for the 175nm wide comb. For applications in optical communications, arbitrary waveform generation, and RF photonics a comb with less power variation is desired. The lesson learned in this section, will be applied to the following experiments to obtain a broadened comb with better power variation. This will be done by obtaining a better quality pulse to be launched into the nonlinear medium.

3. ONE STAGE PULSE APODIZATION IN ONE STAGE OF NONLINEAR PROPAGATION

The underlying principle that flows through this thesis and the work presented in it is the idea that, by apodizing the seed pulse prior to nonlinear propagation, this will return a flat broadened spectrum. This work further reinforces the underlying principle because it was shown that the output pulse and broadened spectrum are strongly influenced by the input pulse profile. Secant hyperbolic (sech), Gaussian, and parabolic input pulses are shown to result in a broad and spectrally flat comb [34].

Traditionally, sech and Gaussian shaped pulse trains at fixed repetition rates were generated by integrated mode-locked lasers. However, recently our group demonstrated a scheme for direct Gaussian comb generation using three intensity modulators and two phase modulators cascaded together to modulate a CW laser [35–37]. When the Gaussian comb is directed into HNLF, it results in substantial spectral broadening, with 3.5 dB power variation within a 28nm bandwidth. However, this comb generation scheme using Gaussian or sech pulses causes spectral sidelobes on either side of the flat spectral region due to wave-breaking [34, 35]. Wave-breaking results from the interference between overlapping frequencies in the leading or trailing edge of the pulse. This will result in rapid temporal modulation of the pulse. These spectral sidelobes have a nonlinear chirp and are not desirable for most applications due to the formations of pedestals around the compressed pulse [35]. Previous work has demonstrated the use of parabolic pulses to seed HNLF and result in spectral broadening. These combs, resulting from parabolic seed pulses, possess a purely linear chirp over the entire bandwidth, due to the fact that parabolic pulses do not suffer from optical wave-breaking [38, 39]. Another beneficial characteristic of these combs is that more power is concentrated in the flat central region [39]. Parabolic pulses generated through passive pulse shapers (e.g. superstructure fiber Bragg grating [38])

or programmable pulse shapers [39], have been spectrally broadened, resulting in 3dB power variation over a 29nm bandwidth and 3dB power variation over a 20nm bandwidth, respectively.

These examples stimulate the work presented in this chapter. Here a simple broadband, and flat comb generation scheme using only an optoelectronic comb source, a programmable pulse shaper, and HNLF are presented. The flat spectral shape of the seed comb generated by the optoelectronic frequency comb source provides a high degree of flexibility for optimizing the input field through pulse shaping. Furthermore, both the temporal profile and the repetition rate of the input pulse to be launched to the HNLF are simultaneously reconfigurable. Using the pulse shaper, Gaussian and parabolic input pulses are generated. The pulses are launched into the HNLF, and a broadband and flat comb showing $< 2dB$ power variation in the flat-topped region is achieved. First, the optoelectronic comb generator scheme will be discussed. After which, the experimental setup and experimental procedure will be presented. The physical phenomena occurring in the HNLF during pulse propagation will be presented.

3.1 Optoelectronic Frequency Comb Source

It was mentioned in the introduction of this thesis that optoelectronic frequency combs are utilized in such applications as optical communications, RF photonics, and optical arbitrary waveform generation [6–9]. The laser source is switched to this because this offers more reconfigurability than the source in Section 2.0. The repetition of the source can be varied in this scheme, allowing for more spacing between comb lines and therefore better resolution when performing pulse shaping. With the newly obtained knowledge on how to compress a pulse, it is believed that this source will provide better pulses for nonlinear propagation. The basic scheme for optoelectronic comb generation is a continuous wave (CW) laser passed through electro-optic modulators that are driven by an external RF source. The modulation induced by the

modulators creates sidebands around the frequency of the input CW laser [40]. The optoelectronic comb source used in the work presented in this chapter employs the single-pass configuration. The single-pass configuration involves cascading these EO modulators together.

The IM is biased to carve out a train of square pulses with a 50% duty cycle. By aligning the PM signal with the IM signal, this will carve pulses from the CW laser. This only occurs when the chirp from the PMs is linear. This linearity provides a flat spectrum. If the temporal signals are correctly aligned in time, the IM will carve the light only when the chirp from the PMs is mostly linear, hence providing a relatively flat spectrum. The PM introduces sidebands around the original input frequency [41].

In order for the PM to modulate the CW laser and create a broad spectrum, the modulation index must be maximized. The modulation index is given in equation 3.1. In this equation v is the amplitude of the voltage of the RF signal driving the modulator and the parameter v_π is a device parameter known as the halfwave voltage. This is the amount of power needed to achieve a π phase shift.

$$\Delta\theta = \frac{\pi v}{v_\pi} \tag{3.1}$$

As stated in [42] an ideal electro-optic modulator should not only have a low v_π parameter, but it should be capable of sustaining high RF power.

Now that we have a better understanding of the background we can move on to the optoelectronic comb generator configuration. The configuration of the optoelectronic comb source can be seen in figure 3.1.

The single-pass configuration results in a frequency comb with output power $>$ 15 dBm and tunability of the repetition rate from 6GHz to 18GHz. This frequency comb output between 60 and 73 lines within 10dB.

The optoelectronic comb generator consists of 3 PMs and 1 IM that are driven by the same RF source. Each modulator has a bandwidth of 20GHz. The first two PMs have the capability of handling RF powers up to 1W with low loss. This leads to an output power up to 15dBm.

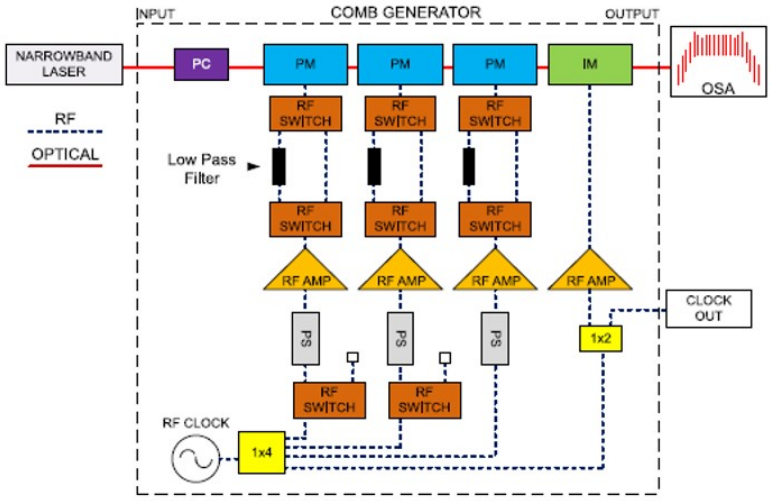

Fig. 3.1. Figure of the optoelectronic frequency comb generator schematic [41]. The schematic shows the single pass configuration that will result in between 60 and 73 lines depending on the repetition rate.

3.2 Experimental Setup

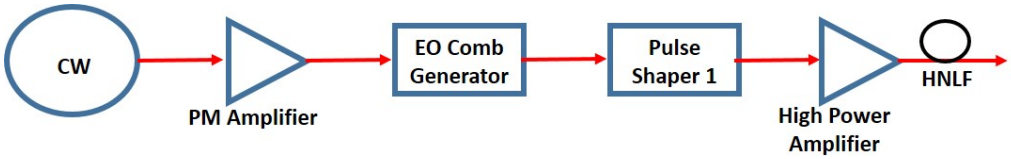

Fig. 3.2. Experimental setup for the one stage pulse apodization in one stage of nonlinear propagation experiments.

The output of the optoelectronic comb source is sent to a programmable Pulse Shaper 1. The pulse shaper is a Finisar WaveShaper 1000S single polarization that has a bandwidth of 30nm. The output of the optoelectronic comb source returns a linear polarization that is aligned to the polarization of the pulse shaper and the EDFA. PM fiber is used to maintain the polarization state while the pulse is propagating through the first part of the system. The pulse shaper allows us to control the spectral amplitude and phase of the frequency comb output by the EO comb source. Using

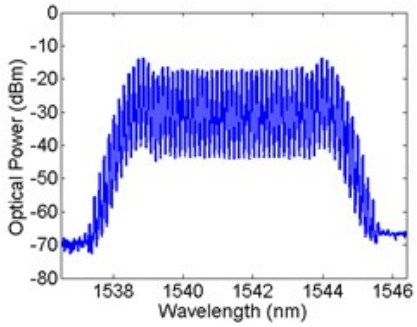

Fig. 3.3. Figure of the 6nm spectrum returned by the optoelectronic frequency comb generator.

the pulse shaper then allows for the apodization of the comb to either a Gaussian or parabolic shape. Therefore, the pulse shaper allows for the main idea of this thesis to be applied, which is that, by apodizing the pulse prior to nonlinear propagation, a flatter comb will be returned.

The output of the pulse shaper is seeded into the EDFA. The EDFA, as the name implies, amplifies the pulse that will be seeded into the HNLF. By amplifying the pulse, its intensity will be increased. Increasing the intensity will allow for more SPM in the HNLF and thus will lead to spectral broadening. Therefore, the output of the EDFA is seeded into HNLF with parameters listed in table 2.1.

The second pulse shaper is used to compensate for the dispersion that is induced on the pulse while propagating through the HNLF. This will be explained further in the next section. An Optical Spectrum Analyzer (OSA) and an Autocorrelator are used to characterize the output of the system.

Let us examine what occurs in the HNLF during spectral broadening.

3.2.1 Normal Group Velocity Dispersion HNLF Spectral Broadening

The use of normal dispersion HNLF was chosen because, as is stated in [34], broadening via normally dispersive fibers leads to a moderate amount of broadening and temporal stability of the output pulses. Before we tackle what is occurring in

the HNLF, let us get a better understanding of group velocity dispersion and in particular, normal group velocity dispersion. A pulse of light is made up of a sum of monochromatic waves. In a dispersive media, the frequency dependent refractive index and absorption coefficient will cause monochromatic waves traveling at different frequencies to propagate at different velocities and undergo different attenuations. Therefore, as a pulse of light travels through a dispersive media, like a fiber, each of the different monochromatic waves making up the light pulse will be modified differently. This will then cause the pulse to be delayed and broadened [17].

3.3 Experimental Results

The following figures show the data from the arbitrary pulse generation section of the experiments.

Figure 3.3 shows the output of the EO comb source. The repetition rate of the comb is 18GHz. Recall that the repetition rate of the comb is determined by the frequency of the RF source driving the modulators. Using the pulse shaper, the quadratic phase of the EO comb can not only be compensated for, but can also apodize the output of the EO comb source.

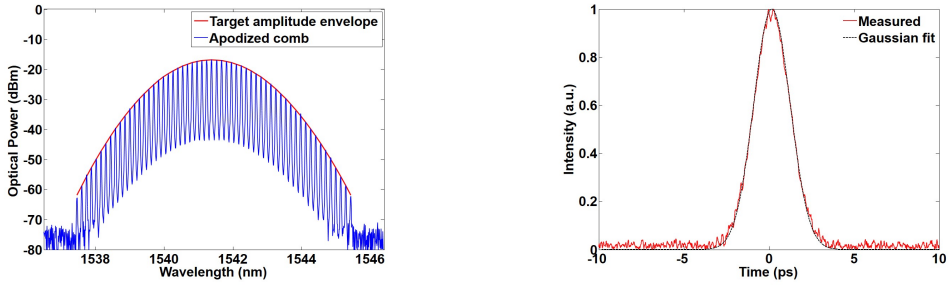

(a) 4nm wide Gaussian apodization.

(b) Compressed Gaussian pulse launched into HNLF.

Fig. 3.4. a. Figure of the 4nm Gaussian apodization performed by the pulse shaper; b. and the compressed Gaussian pulse that is launched into the HNLF.

Figure 3.4a shows the Gaussian apodization of the comb source. The pulse shaper also applies a quadratic phase to compress the pulse returned by the comb source to its bandwidth limit. Figure 3.4b shows the measured autocorrelation (AC) trace at the output of pulse shaper 1. The figure shows two plots, the measured AC trace and the simulated AC trace when the pulse is chirp free. The pulse shaper is used to ensure that a compressed BW-limited pulse is launched into the HNLF. As can be seen in the figure both of these pulses are close to matching and are within the measurement error, therefore the theory and the experiment closely agree. The FWHM of the AC trace is 2.5ps, assuming a Gaussian pulse shape using the deconvolution factor found in [16] of 1.44, this then corresponds to a pulse width of 1.8ps. The Gaussian pulse is amplified by the EDFA and is launched into the HNLF.

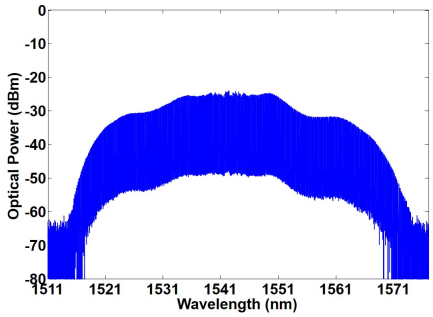

Fig. 3.5. Broadened Gaussian spectrum showing a 1.6dB power variation within a 17nm range

The phase is slightly adjusted to compensate for the chirp that the amplifier introduces to the pulse during propagation. Figure 3.5 shows the broadened spectrum after propagation through HNLF. Recall that the EDFA amplifies the pulse so that its intensity is increased. This increased intensity leads to a larger degree of SPM in the HNLF which leads to increased spectral broadening. The average power of the EDFA was set to 1.17W. This led to a power variation, or spectral ripple, of 1.6dB within an optical bandwidth of 17nm.

3.3.1 Parabolic

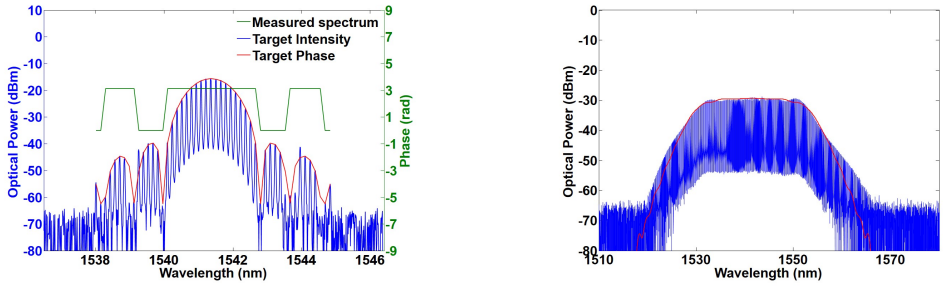

(a) Figure of Parabolic apodization.

(b) Figure of broadened parabolic comb spectrum after HNLF propagation.

Fig. 3.6. a. Figure of the Parabolic apodization performed by the pulse shaper; b. and the corresponding broadened spectrum after HNLF propagation. The resulting power variation is 1.5dB within a 20nm range.

Figure 3.6a shows the parabolic apodization of the optoelectronic comb source. The figure also shows the target spectrum (in red) and the target phase (in green). Note that the spectrum of the parabolic pulse has spectral sidelobes similar to a sinc shape, and the phase difference between two adjacent sidelobes of the apodized spectrum is π. The majority of the frequency components align closely to their target amplitude. In other words, the blue spectrum almost entirely matches the red target spectrum. However, the amplitude of some of the frequency components in the sidelobes deviate slightly from the target intensity due to the dynamic range limitation of the pulse shaper. Figure 3.6b shows the broadened spectrum of the parabolic pulse after propagation in HNLF. The EDFA power level is set to 2.4W. The broadened spectrum has a 1.5 dB power variation within an optical bandwidth of 20nm. Notice the red simulated spectrum demonstrating the theory and the experimental results closely matching.

3.4 Discussion of Experimental Results

As can be seen from the experimental results in the previous section, the parabolic pulse results in a flatter comb with reduced spectral wings, as expected. Previous work has demonstrated that a pulse that is parabolically apodized will resist optical wavebreaking and that a relatively high spectral density is maintained at a long propagation distance [34]. Refer to figure 1.2a for a visualization of the following description. The following description was adapted from [16]. As the pulse continues to propagate, the center up-chirp region will continue to broaden. The fast down-chirp at the leading and trailing edge will sharpen. This will cause the overlap of the frequency components. Optical wavebreaking is not necessarily a detrimental effect, but it certainly induces physical phenomena not wanted in most applications, because after wavebreaking occurs the pulse will undergo significant temporal broadening. This means that the frequencies making up the light pulse will be dispersed. This is an adverse effect not wanted in telecommunications because it is important to control and limit the amount of temporal broadening in order to avoid distortions induced by pulse-to-pulse interactions [34]. This is important because the combination of normal dispersion and nonlinearities will result in dramatic pulse distortion [34]. And it is these distortions that will lead to a comb spectra with lots of ripple. This will lead to degradation in the wings of the broadenend comb spectrum. By shaping the pulse parabolically prior to nonlinear propagation, we can limit the effect of these pulse distortions. In doing so, the flatness of the broadened comb spectrum will be preserved. This can lead to its application in optical communications and arbitrary waveform generation.

Another positive aspect of this setup is the use of normal dispersion HNLF. One detrimental effect that may occur from ultrashort pulses in nonlinear propagation is modulation instability (MI). MI arises from the interplay between SPM and anomalous dispersion that leads to enhancements of small perturbations [43]. By using normal dispersion HNLF, the detrimental effects of instability due to noise are re-

duced because MI does not occur in this type of fiber. But what is more promising is the fact that normal dispersion flattens the noise perturbations [43].

All of the experiments were performed at 18GHz. At this repetition rate, the optoelectronic comb generator will output approximately 60 lines. This repetition rate was chosen for various reasons. At 18GHz, the EO comb source produces a broader comb. This means that more bandwidth is available. And also means shorter pulses can be produced. Also, at this repetition rate the comb lines are spaced further apart, which allows for easier access of each of the spectral lines. This makes using the pulse shaper to apply phase, amplitude, or a combination of both to each spectral line easier because they are spaced further apart.

A flat broadband comb generation technique using an EO comb source, pulse shaper, and HNLF was demonstrated. By shaping the pulse prior to nonlinear propagation, a good spectrally flat comb can be achieved. The next goal is to achieve more bandwidth while maintaining the spectral flatness achieved with this scheme. To do, so another setup in which we use two stages of pulse apodization prior to nonlinear propagation is proposed. By doing this, the spectral flatness should be preserved and more bandwidth should also be achieved. The following section will examine the two stage apodization technique.

4. TWO STAGE PULSE APODIZATION IN TWO STAGES OF NONLINEAR PROPAGATION

The results from the Section 2.0 demonstrated impressive broadening. However, a flatter comb spectra is desired for applications in optical communications [3–5], arbitrary waveform generation [10], and RF photonic filtering [6–9]. But two stages of broadening proved to result in substantial broadening. The scheme in Section 3.0 resulted in a flat spectrum from one stage of pulse apodization. Therefore, the two schemes presented in the previous two chapters will be combined. It has been shown in [18, 19] that two stages of pulse apodization lead to flat broadened comb spectrum. The following experimental setup employs commercially available fibers, pulse shapers, and an in-house built frequency comb generator.

Therefore the new setup will consist of two stages of pulse apodization and nonlinear propagation. Both stages will employ HNLF as the nonlinear propagation medium. The comb source will be the optoelectronic comb generator used in the one stage broadening experiments. The hypothesis is that adding a second stage to the experiments performed in Section 3.0 will result in a flat broadened spectrum. This hypothesis is made because continuum generation in HNLF has been extensively studied [1, 18, 19]. Specifically in [1] different schemes employing HNLF as the broadening technique and their effects were presented. [1] found that these schemes resulted in good spectral broadening. In other work performed by our group, it was found that pulses spectrally broadened in HNLF performed well in optical communication experiments [32]. This work also demonstrated that comb spectra generated via propagation in HNLF possessed better extinction ratio. Also, fibers in the normal dispersion regime do not suffer the detrimental effects of Modulation Instability (MI).

Therefore, in the first stage, the apodization can be implemented. This is advantageous because the work presented in Section 3.0 demonstrated that shaping the

pulse prior to nonlinear propagation resulted in a flat broadened comb spectra. In the second stage, the pulse will be shaped using a parabolic profile prior to nonlinear propagation. It has been previously been discussed that a parabolic pulse undergoing spectral broadening does not undergo optical wave breaking (OWB). If a chirp-free pulse is launched into the HNLF, this will ensure that the parabolic pulse will retain its shape during propagation. And this will lead to a flatter spectral profile after the second stage of broadening. The rest of this chapter will introduce the two stage broadening setup and discuss the expectations of these experiments. Simulation results of these experiments will also be demonstrated. The experimental results will be presented and further discussed.

4.1 Experimental Setup

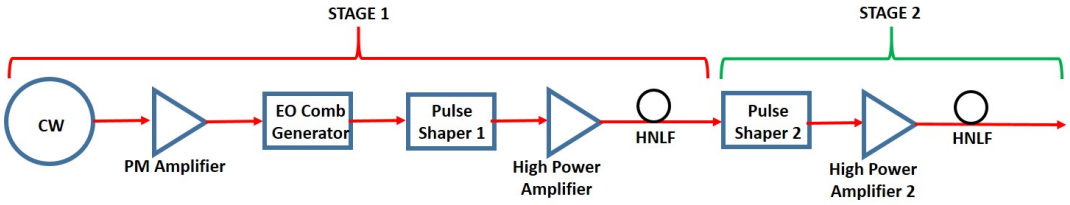

Fig. 4.1. Experimental setup of the two stage pulse apodization in two stages of nonlinear propagation experiments. The setup employs HNLF in both stages of nonlinear propagation.

To gain a better understanding of the experimental setup in figure 4.1, the following section will go step-by-step briefly introducing the components that make up this setup.

4.1.1 Stage 1

The source is a CW laser. The laser used in these experiments is fixed at the wavelength 1542nm. The laser is launched into an amplifier. The amplifier maintains a single polarization throughout propagation. The amplifier is placed before the

optoelectronic comb generator because of the losses it will induce. The maximum input power to the optoelectronic comb generator is 30dBm. The generator will induce approximately 15dB of loss. Therefore, the power at the output of the generator will be approximately 15dBm. After the optoelectronic comb generator, the pulse in launched into the pulse shaper. The first pulse shaper is used to apply a $sech^2$ shape on the pulse. This pulse shape was chosen because it will result in a flatter broadened comb spectrum when compared to a Gaussian shape [39]. The pulse is then launched into an EDFA so as to increase the average power of the pulse. This will increase the SPM occurring in the HNLF. Note that the first stage employs HNLF. In the first experimental setup presented in this work, the first stage employs DDF as the nonlinear medium. Here, the HNLF is used in place of the DDF because the HNLF allows for more spectral broadening. Also, HNLF offers the advantage of being resistant to MI. This was explained in section 3.4.

4.1.2 Stage 2

The pulse enters the second stage via the second pulse shaper. This pulse shaper is used to shape the input pulse into a parabolic profile. The parabolic-shaped pulse is then launched into the second high power amplifier. The nonlinear propagation will take place in a second stage of HNLF. There are limitations in the components of the system that tailor the expectations of the experimental results. For instance, the working range of the pulse shaper is 1527-1567nm. Therefore the bandwidth the first stage generates will be limited by the working range of the second pulse shaper. If the bandwidth is too broad, the second pulse shaper will cut off the spectrum abruptly, causing the loss of bandwidth that was so difficult to obtain. Another limitation is the power the pulse shapers can receive. This is very important in the second stage. The power resulting from the second stage should be below the maximum input power of 0.5W (dB).

4.2 Experimental Results With Simulations

In these simulations, the average power of the pulse propagating through the fiber is initialized. The dispersion and the dispersion slope of the fiber are also initialized so as to calculate and apply the second order and third order dispersion of the fiber. The dispersion D and dispersion slope S can be used to calculate the dispersion as follows.

$$S = (\frac{2\pi c}{\lambda^2})^2\beta_3 + (\frac{4\pi c}{\lambda^3})\beta_2 \tag{4.1}$$

$$D = -\frac{2\pi c}{\lambda^2}\beta_2 \tag{4.2}$$

The higher order dispersion can be applied by modifying the exponential multiplier in the SSFM. Prior to the nonlinear propagation simulation, the HNLF parameters are initialized. The HNLF parameters for the first stage are listed in table 4.1. The HNLF parameters for the second stage are listed in table 2.1.

Table 4.1.
Parameters for HNLF of length of 50m

Parameter	**Value**
Average Power	$P_{AVG} = 2W$
Length of Fiber	$z = 50m$
Dispersion Parameter	$D = -1.88ps/km/nm$
Nonlinear Coefficient	$\gamma = 10.5(Wkm)^{-1}$
Dispersion Slope	$S = 0.016ps/nm^2/nm$

Using these parameters, the second and third order dispersion can be calculated as shown in the previous sections.

Figure 4.2 shows the apodized $sech^2$ after application of the target spectrum, the procedure to do this is introduced in Section 2.0 of this thesis. The bandwidth is 4nm

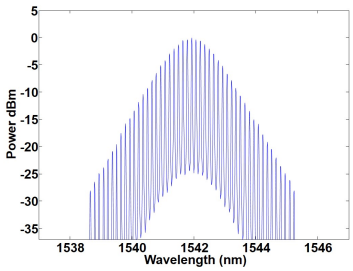

Fig. 4.2. Figure of the 4nm wide apodized $sech^2$ spectrum performed by the pulse shaper.

within 10dB. Figure 4.3a shows the compressed pulse that launched into the first stage of HNLF; the FWHM is approximately 2ps. By applying the deconvolution factor of 1.543, the pulse width is 1.373ps.

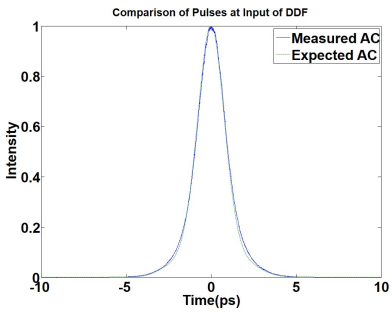

(a) Comparison of the compressed $sech^2$ pulse and the ideal pulse.

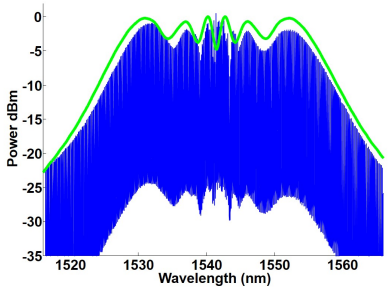

(b) Figure of simulated and experimental broadening after the first stage of HNLF.

Fig. 4.3. a. Figure of the comparison of the ideal and experimental compressed $sech^2$ pulse launched into the first stage of HNLF; b. and the corresponding simulated and experimental broadened comb spectrum after propagation in HNLF with paramaters listed in table 4.1.

Figure 4.3b shows the output of the HNLF with parameters listed in table 4.1. The power of the EDFA was set to 2W and the amount of broadening that results is 34nm within 10dB. This is close to the simulated broadening of 35nm shown by the green spectrum. The parabolic apodization is shown in figure 4.4a. Figure 4.4b shows

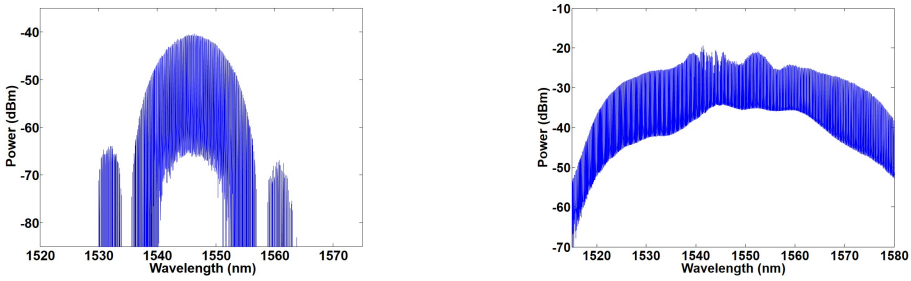

(a) Figure of parabolic apodization.

(b) Figure of broadening after the second stage of HNLF.

Fig. 4.4. a. Figure of the parabolic shaped spectrum performed by the second pulse shaper; b. and the corresponding 58nm wide broadened comb spectrum after the second stage of HNLF with parameters listed in table 2.1.

the broadening achieved is 58nm within 10dB at a power level of 0.5W. The spectral ripple (power variation) is approximately 5dB. The power of the second EDFA was increased to approximately 2W and figure 4.5 shows the spectral broadening. The spectrum is approximately 86nm wide within 10dB. However, notice the most intense central portion of the spectrum has a power variation of approximately 10dB. Because of the greater power variation and the limited input power of 0.5W of the pulse shaper, this comb was not used in the RF photonic filtering experiments. Instead the comb in figure 4.4b was used. The following section explains RF photonic filtering and presents the results of experiments done in collaboration with Dr. Hyoung-Jun Kim.

4.3 RF Photonic Filtering Application

An RF photonic filter implements filtering in the optical domain thus taking advantages offered by photonics. These advantages include low loss inherent to optical fibers, large bandwidths, and immunity to electromagnetic interference, higher operating frequency, tunability, and simpler reconfigurability [44–47].

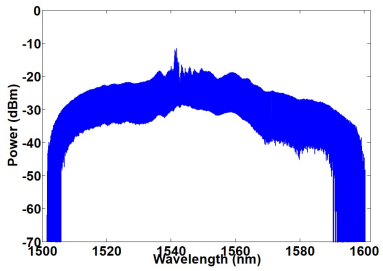

Fig. 4.5. Figure of the spectral broadening achieved after the power of the second EDFA is increased. The spectrum is 86nm wide within 10dB.

RF photonic filters have gained much attention because of the disadvantages suffered from the conventional RF filters. There exist many implementations of RF filters such as MEMS [48] and Solid State Diodes [48]. These types of filters suffer from small RF frequency tuning range, slow tuning speed, slow RF bandwidth reconfiguration, and small Main to Secondary Sidelobe Ratio (MSSR). One of the advantages to microwave photonic filtering is the possibility of achieving larger bandwidths. A larger bandwidth is desired because challenges in RF signal processing are easier to deal with when they are translated to the optical domain [46].

4.3.1 Tapped Delay Line Structure

The implementation of the RF photonic filter we are concerned with is the Tapped Delay Line Structure. Multiple CW lasers at different wavelengths are used as the source. By controlling the power of each of the CW lasers, the weight of each tap can be controlled. The lights at the different wavelengths are combined, and the RF signal is then modulated onto the optical carriers. The optical carriers then travel through a dispersive element that introduces a frequency dependent delay. This delay spreads the different optical carriers, thus making them different filter taps. The optical signal is transformed into an electrical signal via a photodiode. This electrical signal is the output RF signal after filtering. The tapped delay structure

results in a finite impulse response (FIR) filter. This type of filter has the advantage of being flexible in the implementation of both amplitude and phase filters [49, 50]. However, obtaining a large number of taps and controlling their individual weights are difficult to implement. In order to understand the relevant parameters, the RF impulse response for the N-tap RF photonic filter should be introduced. The following derivation is adapted from [51].

$$h(t) = \sum_{n=0}^{N-1} |\mathrm{e}_n|^2 \delta(t - nT) \quad H(\omega) = \sum_{n=0}^{N-1} |\mathrm{e}_n|^2 \mathrm{e}^{-jn\omega T} \tag{4.3}$$

e_n is the electric field amplitude of the Nth tap. And T is the differential delay between the taps. The differential delay is defined in equation 4.4.

$$T = 2\pi \Delta f \Psi_2 \tag{4.4}$$

Ψ_2 is the group delay dispersion and Δf is the spacing between the taps. The differential delay leads to the periodicity of the microwave photonic filter spectrum given in figure 4.6. The period is given by the inverse of the differential delay and it is known as the Free Spectral Range of the filter.

$$FSR = \frac{1}{T} \tag{4.5}$$

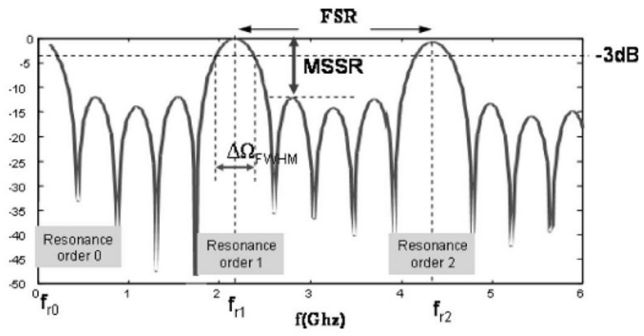

Fig. 4.6. Figure of the Frequency Response of a filter [51] showing important parameters of RF photonic filtering.

Other relevant parameters listed in figure 4.6 [51] are the Main to Secondary Sidelobe Ratio known as MSSR, the Spectral Selectivity which is given by the FWHM at the 3dB point, and the Filter Selectivity that is given by the Q factor.

$$\frac{FSR}{\Delta\Omega_{FWHM}} \tag{4.6}$$

The Q factor is the number of taps used in the implementation of the filter.

A high quality RF photonic filter possesses the ability to tune the RF filtering passband in a large range, a large MSSR, approximately $>$ 30dB, and the ability to reconfigure the RF bandwidth.

4.3.2 Application of Thesis Work To RF Photonic Filtering

By switching the source from an array of CW lasers at different wavelengths to a frequency comb, the system now possesses some advantages. The system now only has one CW source, and the frequency comb offers a large number of taps and tunability. Our group has demonstrated RF photonic filtering employing a frequency comb as the source [7, 8, 52–54]. The implementation of the tapped delay line structure with a frequency comb, as the source varies little from the original implementation presented before. The input RF signal is modulated onto the frequency comb generated in Section 4.0 via a single sideband modulator. This creates a single sideband on each of the individual comb lines. The individual optical carriers then travel through the dispersive fiber. This dispersive fiber induces a different delay on each of the optical carriers, i.e. the individual comb lines. The optical signal is converted back into the RF domain through a photodetector.

Due to the delay induced by the dispersive fiber, the individual comb lines function as independent taps. One of the relevant parameters of a microwave photonic filter is the FSR. The novelty of this scheme is that the FSR of the filter can be varied by changing the length of the dispersive fiber or the repetition rate of the comb.

4.3.3 Results of RF Photonic Filtering

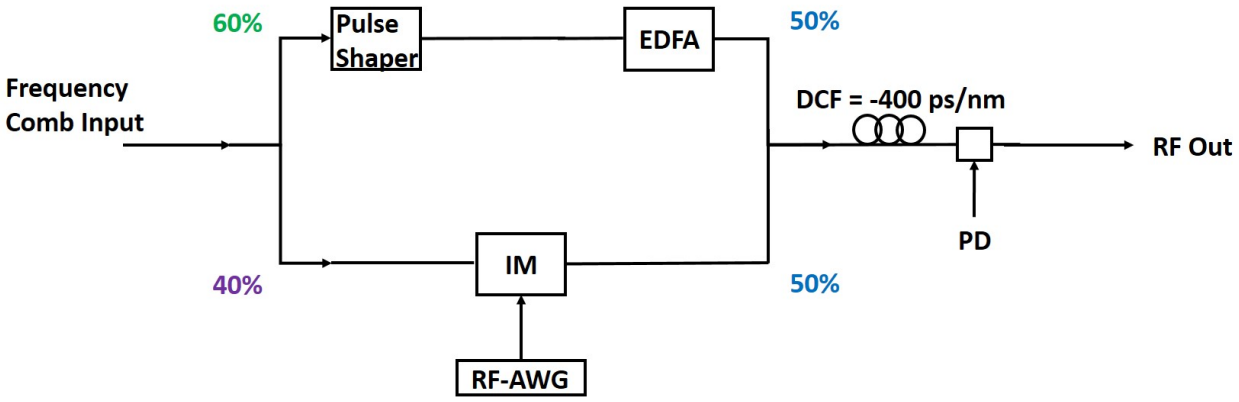

Fig. 4.7. Figure of RF photonic phase filtering scheme that results in pulse compression of input chirp RF waveforms.

The filter implemented in figure 4.7 is a phase filter. With this setup a broadband pulse, also known as a chirp, can be compressed. This is accomplished because only the input signal that is matched to the filter will be compressed and the rest of the signal and noise will be suppressed. A matched filter maximizes the signal-to-noise-ratio (SNR) [55]. Our group has demonstrated the implementation of a matched filter using a pulse shaper for pulse compression [52], and has also demonstrated pulse compression with the use of a 12.8nm wide Gaussian-shaped comb and a repetition rate of 10GHz [53].

The frequency comb shown in figure 4.4b is launched into the filter setup. 60% of the comb signal is split into the upper arm and launched into the pulse shaper. The pulse shaper allows for control of the amplitude of the taps, i.e. frequency comb lines. Also it allows for implementation of the matched filter. Use of the pulse shaper allows for the application of quadratic phase. This will allow for the phase response to be varied and matched to the input RF signal, and thus implementing pulse compression. The other 40% of the comb signal is split into the lower arm and launched into an

IM, and the RF signal to be compressed is modulated onto the comb. The outputs of the different arms are then launched into the Dispersion Compensating Fiber (DCF). The DCF introduces the differential delay defined in equation 4.4. This allows for the two paths, lower and upper arm, to be matched for balanced photodetection. Our group has demonstrated that by employing balanced photodetection the RF gain is increased [54].

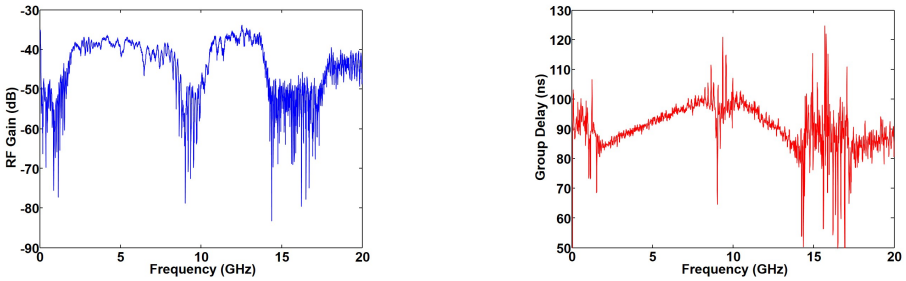

(a) Amplitude response of the RF photonic phase filter.

(b) Group delay response of the RF photonic phase filter.

Fig. 4.8. a. The amplitude response showing the RF bandwidth of 6GHz; b. and delay response of the RF photonic phase filter showing the measured time aperture of 15.3ns.

Figure 4.8a shows the magnitude response and figure 4.8b shows the group delay response of the RF photonic phase filter. The delay response of the system is a measure of the time it takes the signal to travel through the system. It is noted that a linear delay response is needed to compress the linear chirp of the input RF signal.

It is important to show the programmability of the quadratic phase, which allows for the implementation of the matched filter. Figure 4.9 shows the effect of varying the value of quadratic phase that is applied by the pulse shaper in the upper arm of the setup. Figure 4.9a shows that varying the phase allows for the RF bandwidth to be maximized, and in this case it was shown to be 6GHz. Figure 4.9b shows the variability of the group delay response. By varying the value of the quadratic phase applied by the pulse shaper, the phase response of the filter can be matched to the input RF signal. Figure 4.9b also shows the value of dispersion, β, applied by the

pulse shaper. The optical phase applied by the pulse shaper can be represented by $\Phi = \beta n^2$. Where n is the n^{th} comb line.

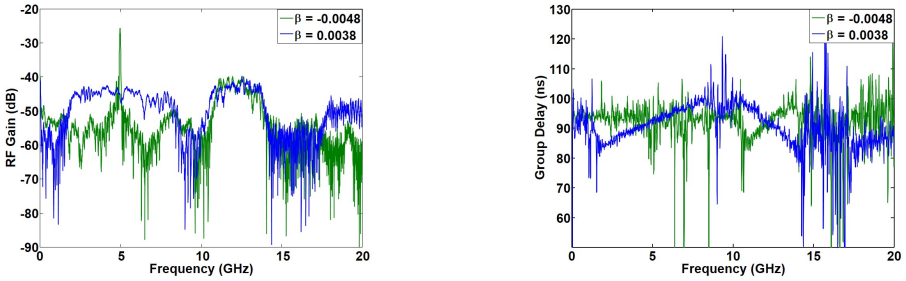

(a) Variability of the magnitude response by varying quadratic phase.

(b) Variability of the group delay response by varying the quadratic phase.

Fig. 4.9. a. The magnitude response of the RF photonic phase filter. By varying the quadratic phase, the RF bandwidth is varied; b. and the group delay response of the RF photonic phase filter. By varying the value of the quadratic phase the phase response can be matched to the input RF signal. The corresponding β value is also listed.

The maximum achievable time aperture of the filter can be determined by obtaining the product of the comb bandwidth and the dispersion induced by the DCF. In this case the dispersion induced is -400 ps/nm. The bandwidth of the comb is approximately 40nm within 10dB. Therefore the maximum achievable time aperture is calculated to be approximately 16ns. However, the measured time aperture is 15.3ns. Pulse compression is limited by the Time Bandwidth Product (TBP); therefore a large TBP is desired. The TBP can be obtained by calculating the product of the RF bandwidth and the time aperture. By analyzing the first filter passband in figure 4.8a the RF bandwidth is determined to be 6GHz. The TBP, assuming the maximum achievable time aperture, is then calculated to be 96. Assuming the measured time aperture, the TBP is calculated to be 91.8.

The TBP is dependent on the bandwidth of the frequency comb [53]. Therefore a larger bandwidth will result in a larger TBP. Recently in our lab, a comb 23nm

wide was used as the source in RF photonic phase filtering. This results in 161 lines. The comb used in the experiments presented in this thesis was 40nm wide. Note that the maximum bandwidth of the pulse shaper in the upper arm is 40nm. This resulted in approximately 276 comb lines. The TBP for the filter with 161 lines was approximately 54. The TBP for the experiments presented in this thesis was calculated to be 91.8. Therefore, the comb with more lines resulted in a greater TBP. If the pulse shaper did not limit the number of comb lines that could be used, the TBP can be further increased.

Figure 4.10a shows two periods of the 14ns input chirp. The input chirp is generated with an electrical RF arbitrary wavefrom generator and modulated onto the frequency comb in the lower arm via the IM. Figure 4.10b shows the measured compressed pulse compared to the ideal autocorrelation trace of one period of the input chirp. This shows that the filter response matches the input chirp well.

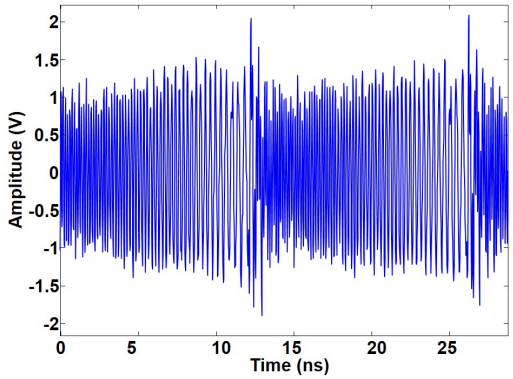

(a) Input 14ns chirp modulated onto the frequency comb via the IM in figure 4.6.

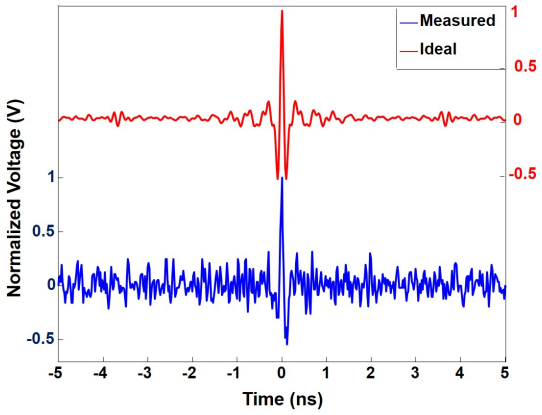

(b) The compressed pulse resulting from the RF photonic phase filter (blue dashed curve) compared to the ideal compressed pulse (red curve).

Fig. 4.10. a. Figure of two periods of the input 14ns chirp RF waveform generated by an electrical RF arbitrary waveform generator; b. and the corresponding compressed chirp, demonstrating that the filter response matches the input chirp well.

5. SUMMARIZATION AND CONCLUSIONS

Table 5.1.
Summarization of the spectral broadening achieved by the different experimental implementations.

Experimental Setup	**Power Variation**
Setup 1 with DDF spectral dip	10dB within 130nm
Setup 1 without DDF spectral dip	5dB within 175nm
Setup 2 Gaussian apodization	1.6dB within 17nm
Setup 2 parabolic apodization	1.5dB within 20nm
Setup 3 second stage parabolic apodization	5dB within 58 nm

5.1 Pulse Apodization In Two Stages Of Nonlinear Propagation

These experiments led to impressive broadening. A MLL was used as the laser source. DDF was used to obtain a compressed pulse via ASC. This pulse was launched into the second stage, in which normal dispersion HNLF was used as the nonlinear medium. A 130nm wide comb was generated. However, after a smoother spectrum was generated at the output of the DDF, a 175nm wide comb was generated. However, a comb with less power variation was desired. The main lesson learned here was that care must be taken in generating the pulse that is to be launched into the nonlinear medium. A pulse that is not chirp free will result in degradation of the broadened comb spectrum. In these experiments, it was difficult to overcome the higher order phase induced by propagation in the EDFA and this also led to degrada-

tion in the broadened comb spectrum. These lessons were applied in the experiments that followed.

5.2 One Stage Pulse Apodization In One Stage Of Nonlinear Propagation

Gaussian and parabolic apodization led to flat broadened comb spectrums after propagation in one stage of nonlinear propagation in HNLF. The Gaussian spectrum led to a sub 1.6dB power variation within a 17nm range. The parabolic spectrum returned a broadened comb spectrum 20nm wide with a sub 1.5dB. The laser source was switched from the MLL in the first experiments to the optoelectronic frequency comb generator. This was done because the source is more reconfigurable and allows for the repetition rate to be varied.

5.3 Two Stage Pulse Apodization In Two Stages Of Nonlinear Propagation

In these experiments, a broadened comb spectrum with a power variation of 5dB was generated. The setup implemented used two stages of normal dispersion HNLF. In the first stage, a $sech^2$ shape was implemented. The resaon being a $sech^2$ shaped pulse results in a flatter broadened spectrum. This generates a 34nm wide comb within 10dB. This shows that the first stage produces more spectral broadening when compared to the broadening produced by the DDF in the first stage of the first experimental setup. Also this offers more stability than the first experimental setup. The second stage shapes the broadened spectrum into a parabolic shape. The parabolic pulse will result in a flat broadened spectrum because it resists OWB. After propagation in the second stage of HNLF, a 58nm wide comb within 10dB is generated. This comb was then used in RF photonic phase filtering. By varying the quadratic phase applied by a pulse shaper, the phase response of the filter can be matched to input RF signal. This will allow for pulse compression. A 14ns chirp is compressed

and the comparison of the ideal autocorrelation trace and the measured compressed pulse show that the filter response matches the input chirp well.

REFERENCES

REFERENCES

[1] T. Yang, J. Dong, S. Liao, D. Huang, and X. Zhang, "Comparison analysis of optical frequency comb generation with nonlinear effects in highly nonlinear fibers," *Optics express*, vol. 21, no. 7, pp. 8508–8520, 2013.

[2] T. Udem, R. Holzwarth, and T. W. Hänsch, "Optical frequency metrology," *Nature*, vol. 416, no. 6877, pp. 233–237, 2002.

[3] A. D. Ellis and F. G. Gunning, "Spectral density enhancement using coherent wdm," *Photonics Technology Letters, IEEE*, vol. 17, no. 2, pp. 504–506, 2005.

[4] P. J. Delfyett, S. Gee, M.-T. Choi, H. Izadpanah, W. Lee, S. Ozharar, F. Quinlan, and T. Yilmaz, "Optical frequency combs from semiconductor lasers and applications in ultrawideband signal processing and communications," *Lightwave Technology, Journal of*, vol. 24, no. 7, pp. 2701–2719, 2006.

[5] D. Hillerkuss, R. Schmogrow, T. Schellinger, M. Jordan, M. Winter, G. Huber, T. Vallaitis, R. Bonk, P. Kleinow, F. Frey *et al.*, "26 tbit s-1 line-rate superchannel transmission utilizing all-optical fast fourier transform processing," *Nature Photonics*, vol. 5, no. 6, pp. 364–371, 2011.

[6] C.-B. Huang, D. E. Leaird, and A. M. Weiner, "Time-multiplexed photonically enabled radio-frequency arbitrary waveform generation with 100 ps transitions," *Optics letters*, vol. 32, no. 22, pp. 3242–3244, 2007.

[7] E. Hamidi, D. E. Leaird, and A. M. Weiner, "Tunable programmable microwave photonic filters based on an optical frequency comb," *Microwave Theory and Techniques, IEEE Transactions on*, vol. 58, no. 11, pp. 3269–3278, 2010.

[8] V. Supradeepa, C. M. Long, R. Wu, F. Ferdous, E. Hamidi, D. E. Leaird, and A. M. Weiner, "Comb-based radiofrequency photonic filters with rapid tunability and high selectivity," *Nature Photonics*, vol. 6, no. 3, pp. 186–194, 2012.

[9] M. Song, A. J. Metcalf, A. M. Weiner *et al.*, "Multitap microwave photonic filters with programmable phase response via optical frequency comb shaping," *Optics letters*, vol. 37, no. 5, pp. 845–847, 2012.

[10] Z. Jiang, C.-B. Huang, D. E. Leaird, and A. M. Weiner, "Optical arbitrary waveform processing of more than 100 spectral comb lines," *Nature Photonics*, vol. 1, no. 8, pp. 463–467, 2007.

[11] J. Hecht. (2012) Photonic frontiers: Frequency combs: Frequency combs make their way to the masses. [Online]. Available: http://www.laserfocusworld.com/articles/print/volume-48/issue-01/features/frequency-combs-make-their-way-to-the-masses.html

[12] N. R. Newbury, "Searching for applications with a fine-tooth comb," *Nature photonics*, vol. 5, no. 4, pp. 186–188, 2011.

[13] M. Kourogi, K. Nakagawa, and M. Ohtsu, "Wide-span optical frequency comb generator for accurate optical frequency difference measurement," *Quantum Electronics, IEEE Journal of*, vol. 29, no. 10, pp. 2693–2701, 1993.

[14] R. W. Boyd, *Nonlinear optics*. Academic press, 2003.

[15] E. Boutet. (2007) Self-phase modulation. [Online]. Available: http://en.wikipedia.org/wiki/Self-phase-modulation

[16] A. Weiner, *Ultrafast optics*. John Wiley & Sons, 2011, vol. 72.

[17] B. Saleh and M. Teich, *Fundamental of photonics, ch 14*. John Wiley & Sons, New York, 1991.

[18] V. Ataie, B. P.-P. Kuo, E. Myslivets, and S. Radic, "Generation of 1500-tone, 120nm-wide ultraflat frequency comb by single cw source," in *National Fiber Optic Engineers Conference*. Optical Society of America, 2013, pp. PDP5C–1.

[19] V. Ataie, E. Myslivets, B. P.-P. Kuo, N. Alic, and S. Radic, "Spectrally equalized frequency comb generation in multistage parametric mixer with nonlinear pulse shaping," *Journal of Lightwave Technology*, vol. 32, no. 4, pp. 840–846, 2014.

[20] S. V. Chernikov, D. Richardson, D. Payne, and E. Dianov, "Soliton pulse compression in dispersion-decreasing fiber," *Optics letters*, vol. 18, no. 7, pp. 476–478, 1993.

[21] S. V. Chernikov and P. V. Mamyshev, "Femtosecond soliton propagation in fibers with slowly decreasing dispersion," *JOSA B*, vol. 8, no. 8, pp. 1633–1641, 1991.

[22] T. Okuno, M. Hirano, T. Nakanishi, and M. Onishi, "Highly–nonlinear optical fibers and their applications," *SEI technical review.–Sumitomo electric Industries*, no. 62, pp. 35–39, 2006.

[23] A. M. Weiner, J. P. Heritage, and E. M. Kirschner, "High resolution femtosecond pulse shaping," *J. Opt. Soc. Amer*, pp. 1563–1572, 1988.

[24] O. V. Sinkin, R. Holzlöhner, J. Zweck, and C. R. Menyuk, "Optimization of the split-step fourier method in modeling optical-fiber communications systems," *Journal of lightwave technology*, vol. 21, no. 1, p. 61, 2003.

[25] G. P. Agrawal, *Nonlinear fiber optics*. Academic press, 2007.

[26] A. Hasegawa, "Optical solitons in fibers for communication systems," *Opt. Photon. News*, vol. 13, no. 2, pp. 33–37, 2002.

[27] C. Menyuk, "Application of multiple-length-scale methods to the study of optical fiber transmission," *Journal of Engineering Mathematics*, vol. 36, no. 1-2, pp. 113–136, 1999.

[28] A. M. Weiner, "Femtosecond pulse shaping using spatial light modulators," *Review of scientific instruments*, vol. 71, no. 5, pp. 1929–1960, 2000.

[29] A. Weiner, "Ultrafast optical pulse shaping: A tutorial review," *Optics Communications*, vol. 284, no. 15, pp. 3669–3692, 2011.

[30] P. Maine, D. Strickland, P. Bado, M. Pessot, and G. Mourou, "Generation of ultrahigh peak power pulses by chirped pulse amplification," *Quantum electronics, IEEE Journal of*, vol. 24, no. 2, pp. 398–403, 1988.

[31] X. Yang, D. J. Richardson, and P. Petropoulos, "Nonlinear generation of ultra-flat broadened spectrum based on adaptive pulse shaping," *Journal of Lightwave Technology*, vol. 30, no. 12, pp. 1971–1977, 2012.

[32] C.-B. Huang, S.-G. Park, D. E. Leaird, and A. M. Weiner, "Nonlinearly broadened phase-modulated continuous-wave laser frequency combs characterized using dpsk decoding," *Optics express*, vol. 16, no. 4, pp. 2520–2527, 2008.

[33] K. Tamura and M. Nakazawa, "Femtosecond soliton generation over a 32-nm wavelength range using a dispersion-flattened dispersion-decreasing fiber," *Photonics Technology Letters, IEEE*, vol. 11, no. 3, pp. 319–321, 1999.

[34] C. Finot, B. Kibler, L. Provost, S. Wabnitz *et al.*, "Beneficial impact of wave-breaking for coherent continuum formation in normally dispersive nonlinear fibers," *JOSA B*, vol. 25, no. 11, pp. 1938–1948, 2008.

[35] R. Wu, D. E. Leaird, A. M. Weiner *et al.*, "Supercontinuum-based 10-ghz flat-topped optical frequency comb generation," *Optics express*, vol. 21, no. 5, pp. 6045–6052, 2013.

[36] R. Wu, C. M. Long, D. E. Leaird, and A. M. Weiner, "Directly generated gaussian-shaped optical frequency comb for microwave photonic filtering and picosecond pulse generation," *Photonics Technology Letters, IEEE*, vol. 24, no. 17, pp. 1484–1486, 2012.

[37] R. Wu, V. Supradeepa, C. M. Long, D. E. Leaird, and A. M. Weiner, "Generation of very flat optical frequency combs from continuous-wave lasers using cascaded intensity and phase modulators driven by tailored radio frequency waveforms," *Optics letters*, vol. 35, no. 19, pp. 3234–3236, 2010.

[38] F. Parmigiani, C. Finot, K. Mukasa, M. Ibsen, M. A. Roelens, P. Petropoulos, and D. J. Richardson, "Ultra-flat spm-broadened spectra in a highly nonlinear fiber using parabolic pulses formed in a fiber bragg grating," *Optics Express*, vol. 14, no. 17, pp. 7617–7622, 2006.

[39] A. M. Clarke, D. G. Williams, M. A. Roelens, and B. J. Eggleton, "Reconfigurable optical pulse generator employing a fourier-domain programmable optical processor," *Journal of Lightwave Technology*, vol. 28, no. 1, pp. 97–103, 2010.

[40] H. Murata, A. Morimoto, T. Kobayashi, and S. Yamamoto, "Optical pulse generation by electrooptic-modulation method and its application to integrated ultrashort pulse generators," *Selected Topics in Quantum Electronics, IEEE Journal of*, vol. 6, no. 6, pp. 1325–1331, 2000.

[41] A. J. Metcalf, V. Torres-Company, D. E. Leaird, and A. M. Weiner, "High-power broadly tunable electrooptic frequency comb generator," *Selected Topics in Quantum Electronics, IEEE Journal of*, vol. 19, no. 6, pp. 231–236, 2013.

[42] V. Torres-Company and A. M. Weiner, "Optical frequency comb technology for ultra-broadband radio-frequency photonics," *Laser & Photonics Reviews*, vol. 8, no. 3, pp. 368–393, 2014.

[43] K. R. Tamura, H. Kuhota, and M. Nakazawa, "Fundamentals of stable continuum generation at high repetition rates," *Quantum Electronics, IEEE Journal of*, vol. 36, no. 7, pp. 773–779, 2000.

[44] A. J. Seeds, "Microwave photonics," *Microwave Theory and Techniques, IEEE Transactions on*, vol. 50, no. 3, pp. 877–887, 2002.

[45] J. Capmany, B. Ortega, D. Pastor, and S. Sales, "Discrete-time optical processing of microwave signals," *Journal of Lightwave Technology*, vol. 23, no. 2, p. 702, 2005.

[46] J. Capmany, "Microwave signal processing using optics," in *Optical Fiber Communication Conference*. Optical Society of America, 2005, p. OThB1.

[47] K. P. Jackson, S. A. Newton, B. Moslehi, M. Tur, C. C. Cutler, J. W. Goodman, and H. Shaw, "Optical fiber delay-line signal processing," *Microwave Theory and Techniques, IEEE Transactions on*, vol. 33, no. 3, pp. 193–210, 1985.

[48] G. M. Rebeiz, *RF MEMS: theory, design, and technology*. John Wiley & Sons, 2004.

[49] C. K. Madsen and J. H. Zhao, *Optical filter design and analysis*. Wiley-Interscience, 1999.

[50] F. J. Harris, "On the use of windows for harmonic analysis with the discrete fourier transform," *Proceedings of the IEEE*, vol. 66, no. 1, pp. 51–83, 1978.

[51] J. Capmany, B. Ortega, and D. Pastor, "A tutorial on microwave photonic filters," *Journal of Lightwave Technology*, vol. 24, no. 1, p. 201, 2006.

[52] E. Hamidi and A. M. Weiner, "Phase-only matched filtering of ultrawideband arbitrary microwave waveforms via optical pulse shaping," *Journal of Lightwave Technology*, vol. 26, no. 15, pp. 2355–2363, 2008.

[53] M. Song, R. Wu, A. J. Metcalf, A. M. Weiner *et al.*, "Compression of ultra-long microwave pulses using programmable microwave photonic phase filtering with >100 complex-coefficient taps," *Optics express*, vol. 22, no. 6, pp. 6329–6338, 2014.

[54] H.-J. Kim, D. E. Leaird, A. J. Metcalf, and A. M. Weiner, "Comb-based rf photonic filters based on interferometric configuration and balanced detection," *Journal of Lightwave Technology*, vol. 32, no. 20, pp. 3478–3488, 2014.

[55] G. L. Turin, "An introduction to digitial matched filters," *Proceedings of the IEEE*, vol. 64, no. 7, pp. 1092–1112, 1976.

[56] A. Technologies. (2012) Understanding the fundamental principles of vector network analysis. [Online]. Available: http://cp.literature.agilent.com/litweb/pdf/5965-7707E.pdf

[57] J. Azaña, "Time-to-frequency conversion using a single time lens," *Optics communications*, vol. 217, no. 1, pp. 205–209, 2003.

[58] M. Song, C. M. Long, R. Wu, D. Seo, D. E. Leaird, and A. M. Weiner, "Reconfigurable and tunable flat-top microwave photonic filters utilizing optical frequency combs," *Photonics Technology Letters, IEEE*, vol. 23, no. 21, pp. 1618–1620, 2011.